IJARAI

International Journal of
Advanced Research in Artificial Intelligence

Volume 4 Issue 9

IJARAI

INTERNATIONAL JOURNAL OF ADVANCED RESEARCH IN ARTIFICIAL INTELLIGENCE

Editorial Preface

From the Desk of Managing Editor...

Artificial Intelligence is hardly a new idea. Human likenesses, with the ability to act as human, dates back to Geek mythology with Pygmalion's ivory statue or the bronze robot of Hephaestus. However, with innovations in the technological world, AI is undergoing a renaissance that is giving way to new channels of creativity.

The study and pursuit of creating artificial intelligence is more than designing a system that can beat grand masters at chess or win endless rounds of Jeopardy!. Instead, the journey of discovery has more real-life applications than could be expected. While it may seem like it is out of a science fiction novel, work in the field of AI can be used to perfect face recognition software or be used to design a fully functioning neural network.

At the International Journal of Advanced Research in Artificial Intelligence, we strive to disseminate proposals for new ways of looking at problems related to AI. This includes being able to provide demonstrations of effectiveness in this field. We also look for papers that have real-life applications complete with descriptions of scenarios, solutions, and in-depth evaluations of the techniques being utilized.

Our mission is to be one of the most respected publications in the field and engage in the ubiquitous spread of knowledge with effectiveness to a wide audience. It is why all of articles are open access and available view at any time.

IJARAI strives to include articles of both research and innovative applications of AI from all over the world. It is our goal to bring together researchers, professors, and students to share ideas, problems, and solution relating to artificial intelligence and application with its convergence strategies. We would like to express our gratitude to all authors, whose research results have been published in our journal, as well as our referees for their in-depth evaluations.

We hope that this journal will inspire and educate. For those who may be enticed to submit papers, thank you for sharing your wisdom.

Editorial Board

Reviewer Board Members

- **ISMAIL YUSUF**
  Lamintang Education & Training (LET) Centre
- **Jabar Yousif**
  Faculty of computing and Information Technology, Sohar University, Oman
- **Jatinderkumar Saini**
  Narmada College of Computer Application, Bharuch
- **José Santos Reyes**
  University of A Coruña (Spain)
- **Kamran Kowsari**
  The George Washington University
- **Krasimir Yordzhev**
  South-West University, Faculty of Mathematics and Natural Sciences, Blagoevgrad, Bulgaria
- **Krishna Prasad Miyapuram**
  University of Trento
- **Le Li**
  University of Waterloo
- **Leon Abdillah**
  Bina Darma University
- **Liming Chen**
  De Montfort University
- **Ljubomir Jerinic**
  University of Novi Sad, Faculty of Sciences, Department of Mathematics and Computer Science
- **M. Reza Mashinchi**
  Research Fellow
- **madjid khalilian**
- **Malack Oteri**
  jkuat
- **Marek Reformat**
  University of Alberta
- **Md. Zia Ur Rahman**
  Narasaraopeta Engg. College, Narasaraopeta
- **Mehdi Bahrami**
  University of California, Merced
- **Mohamed Najeh LAKHOUA**
  ESTI, University of Carthage
- **Mohammad Haghighat**
  University of Miami
- **Mohd Ashraf Ahmad**
  Universiti Malaysia Pahang

- **Mohd Helmy Abd Wahab**
  Universiti Tun Hussein Onn Malaysia
- **Mokhtar Beldjehem**
  University of Ottawa
- **Nagy Darwish**
  Department of Computer and Information Sciences, Institute of Statistical Studies and Researches, Cairo University
- **Nestor Velasco-Bermeo**
  UPFIM, Mexican Society of Artificial Intelligence
- **Nidhi Arora**
  M.C.A. Institute, Ganpat University
- **Olawande Daramola**
  Covenant University
- **Omaima Al-Allaf**
  Asesstant Professor
- **Parminder Kang**
  De Montfort University, Leicester, UK
- **PRASUN CHAKRABARTI**
  Sir Padampat Singhania University
- **Qifeng Qiao**
  University of Virginia
- **raja boddu**
  LENORA COLLEGE OF ENGINEERNG
- **Rajesh Kumar**
  National University of Singapore
- **Rashad Al-Jawfi**
  Ibb university
- **RAVINDRA CHANGALA**
- **Reza Fazel-Rezai**
  Electrical Engineering Department, University of North Dakota
- **Said Ghoniemy**
  Taif University
- **Said Jadid Abdulkadir**
- **Secui Calin**
  University of Oradea
- **Selem Charfi**
  University of Pays and Pays de l'Adour
- **Shahab Shamshirband**
  University of Malaya
- **Shaidah Jusoh**
- **Shriniwas Chavan**
  MSS's Arts, Commerce and Science College
- **Sim-Hui Tee**

CONTENTS

Case-based Reasoning with Input Text Processing to Diagnose Mood [Affective] Disorders

Sri Mulyana, Sri Hartati, Retantyo Wardoyo, Edi Winarko
Department of Computer Sciences and Electronics
Gadjah Mada University
Yogyakarta, Indonesia

Abstract—**Case-Based Reasoning is one of the methods used in expert systems. Calculation of similarity degree among the cases has always been an important aspect in CBR as the system will attempt to identify cases with the highest of similarity degree in a case-base to provide solutions for new problems. In this research, a CBR model with input text processing for diagnosing mood [affective] disorder is developed. It correlates with the increased tendency of mood disorder in accordance with the dynamics of the economic and political situation.**

Calculation of similarity degree among the cases is one of the main focuses in this research. This study proposed a new method to calculate similarity degree between cases, Modified-Tversky. The analysis performed to assess the method used in measuring case similarity reveals that the Modified-Tversky Method surpasses the other methods. In the all tests conducted, the results of case similarity measures using the Modified-Tversky method is greater than or equal to the calculations performed using the Jaccard dan Tversky methods. The test results also provide an average level of performance in processing text input is 89.3 %.

Keywords—Case-Based Reasoning; mood disorder; case similarity; Jaccard Method; Tversky Method; Modified-Tversky Method

I. INTRODUCTION

Case-Based Reasoning (CBR) is a method adopted from knowledge-based system in various domains. The method uses experiences from previous similar cases to solve new problems. The main idea is the assumption that similar cases have similar solutions [1].

The development of CBR possesses vast research opportunities including those related to case similarity calculation algorithms, indexing techniques to increase the efficiency of retrieval processes, case representation techniques, and methods to append new cases to the case base [2].

Researches could also be conducted by combining existing techniques through improvement or addition of new algorithms to achieve a need-fulfilling case-based computerized reasoning system. To test the validity of the techniques developed, implementation in a certain field is required.

In this research, a CBR model to diagnose mood [affective] disorder is developed. Mood [affective] disorder is caused by the inability of an individual to adapt to social evolution. There is an increased tendency of mood disorder parallel to economic and political change.

That choice of field of implementation is based on the increased tendency of mood disorder due to the occurance of economic and political change. The cause is the inability of an individual to adapt to social evolution.

In life, every single human being exhibits different kinds of emotions. Those expressions and feelings vary and is usually temporary, but could pose a problem if not immediately treated, resulting in emotional disorder including heavy depression rendering the subject devoid of motivation, happiness, and empathy.

Bitter experiences could cause an individual to feel insecure, void, depressed, and even hateful. That in turn results in uncontrollable anger planted deeply in one's inner conscience. What is felt as an unpleasant experience leads to extreme grief and all other forms of depression [3]. This condition could formulate as a chronic and repetitive problem interfering with an individual's ability to live out his every-day responsibilities.

II. CBR RESEARCH IN HEALTH

The application of CBR has been vastly developed in various fields, particularly in health. Those is deployed to diagnose infection related diseases [4]. Explained in those researches is that such cases possess certain attributes such as temperature, headaches including its intensity and area of effect, coughing, bowel movement frequency, nausea, and urination. All those attributes have a numerical value in a scale of 1 to 4 to represent its intensity ranging from none or never, low, average, and high. Euclidean distance is employed in this research to measure similarity degrees between cases.

Current ongoing researches show that the implementation of CBR in the medical field has seen great development. Chakraborty at al. introduced a CBR system to detect swine flu dubbed SFDA (*Swine Flu Diagnostic Assistant*) [5], and Tomar at al. developed a CBR system to diagnose heart attacks [6]. Pant and Joshi have also done the same in the field of neurology in the form of NDS (*Neurology Diagnosis System*) [7]. The method used to measure similarity was the Nearest-neighbor method. Other CBR-based system was developed to advertise the dangers of smoking. It contained early warnings about the health effects of smoking broadcasted through mobile phones [8].

In the future, CBR systems could help provide better services in the medical field and perhaps have tighter integration with the clinical environment.

III. MOOD [AFFECTIVE] DISORDERS

An individual's mood is the internal emotion that he or she dominantly feels, affects one's behavior and perception, and tends to be stable for a period of time. On the other hand, an affect is an external expression of a mood. Moods can be in a normal state, increasing, and deppressive. A healthy mind has a wide range of moods, a good balance of affect expression, and is able to control mood and affects [9]. Mood disorders are triggered by extreme and uncontrollable mood fluctuation, resulting in a lack of adaptive ability, and could cause difficulty or discomfort.

Mood disorders are emotional illnesses accompanied by symptoms of mania and depression [10]. It is the result of the presence of complete negativity in an individual's mind, where said individual views himself, life, and the future as a chaotic mess of failure. Someone experiencing such a mood [affective] disorder would feel a lack of connection with other people or devoid of an influential role in their lives [3].

Mania is a certain mood disorder indicated by an abnormal increase of a certain mood. This condition is also accompanied by behavioral symptoms in the form of over-activity, talkativeness, great enthusiasm, euphoria, and even sexual deviation [10]. There exists two groups of maniacal symptoms, one being euphoric (elation, increased enthusiasm, heightened optimism), and the other being irritability (anger, aggressiveness, and violence). Hypomania is the condition of a slightly lower increase of mood compared to mania, and that usually does not reach the level where day to day functionality is threatened. Related to the time needed for diagnosis, hypomania can be identified as quickly as four days since the symptoms arrive [11].

Depression is a common emotional disorder indicated by constant sadness, loss of desire, a feeling of guilt, insecurity, sleeping problems or a decrease of appetite, low enthusiasm and energy, and lack of concentration [10]. It can also be associated with continuous grief in a dangerous amount, and is the most common emotional disorder. One in seven all around the globe have experienced an episode of depression at least once in their lives. It is the most common cause of death in developed nations and is the fourth most common cause in developing countries. Bipolar disorder is a chronic type of mood disorder with recurring episodes of mania or hypomania that strikes in turn with depression [11]. It also includes depression symptoms major or minor, usually identifiable by regression or even loss of ability to feel happy and positive during fun activities. This is constantly felt every day for at least two weeks [11]. People suffering from bipolar disorder can appear as overly optimistic individuals, frequently boasting about themselves, and even to the extent of making dangerous or risky decisions without calculating drawbacks and consequences. Sometimes those individuals can turn up brilliant ideas with the need for it to be immediately fulfilled. Unfortunately, those ideas tend to end in failure because of lack of thought, preparation, and some are just too unrealistic.

As a result of their easily irritable mood and the tendency to be easily offended in a state of either mania or depression, those with bipolar disorder often experience interpersonal communication problems with family and people around them. Sometimes they suspect that others are envious of them, and endeavor to prevent those bipolar individuals from achieving great things. During episodes of depression, they tend to blame family members and close friends as the root of their failure and suffering because in their minds they think that they are not provided with enough love, care, and support.

IV. TEXT PROCESSING

Text processing is often required to simplify search process. The main objective is to convert various word forms into much more consistent index terms. An *Index term* is the representation of the essence of a document needed for search purposes. Text processing includes:

a) *Information Extraction: extracting important information within a document.*

b) *Text Summarization: to automatically produce a summary of a document.*

c) *Data Mining: A validation identification process to understand data patterns recorded in a structured database.*

d) *Text Mining: also known as text data mining or information searching.*

e) *Information retrieval: a document search.*

f) *Document Clustering: similar to document classification, but document class is not determined beforehand.*

The steps to process a document text is usually specific according to the process that needs to be carried out. One of the steps of processing a text document is indexing. The aim is to identify the best term to represent a certain document, so during document processing it could be obtained accurately. Automatic indexing consists of:

1) *Tokenization: a stage of processing where the input text is divided into units or "tokens" in the forms of words, numbers or punctuation marks.*

2) *Deletion of stop words: erasing less meaningful words. The choice of stop words are assessed using specific dictionaries, or lists of stops words.*

3) *Synonym identification: locating synonyms from words obtained from a document. This can be conducted with the use of a thesaurus or other similar methods. Similar words can be replaced with general terms.*

4) *Stemming: The process of text normalization within a document or changing an expression to its simplest form that in a literal view may not have a concrete meaning [12].*

5) *Frequency measures of stemming results: One of the methods that can be applied is the n-gram or a series of linguistic n item orders. Those items can be in the form of letters, vocabulary, or words. It is one of the implementations basic word features used in machine learning [13].*

6) *Selection or comparison of word frequency measure results.*

V. CALCULATION OF CASE SIMILARITY DEGREE

Let $\mathrm{Sim}(X, Y)$ denotes the similarity between two cases X dan Y where each have a finite number of features. The following are techniques to calculate the similarity degree:

1) Jaccard Method [14]

Case similarity using the Jaccard Method can be formulated as:

$$\mathrm{Sim}(X, Y) = \frac{|X \cap Y|}{|X \cup Y|} \qquad (1)$$

which also means :

$$\mathrm{Sim}(X, Y) = \frac{\#SAME(X,Y)}{\#SAME(X,Y) + \#DIFFER(X,Y)} \qquad (2)$$

Where:

$\#SAME(X,Y)$: The number of same features between X and Y

$\#DIFFER(X,Y)$: The number of different features between X and Y

This decision usually requires a specific threshold to state that the features of both cases are same or not.

2) Tversky Method[15]

Case similarity with the original Tversky method can be formulated as:

$$\mathrm{Sim}(X, Y) = \frac{\alpha|X \cap Y|}{\alpha|X \cap Y| + \beta|X \oplus Y|} \qquad (3)$$

Where:

$$|X \oplus Y| = |X \cup Y| - |X \cap Y| \qquad (4)$$

which also means :

$$\mathrm{Sim}(X, Y) = \frac{\alpha(\#SAME(X,Y))}{\alpha(\#SAME(X,Y)) + \beta(\#DIFFER(X,Y))} \qquad (5)$$

The value of α dan β is parallel with their respective significance of value, usually formulated by experts or produced using machine based learning techniques.

3) Modified-Tversky Method

The Modified-Tversky Method is a modification of the Tversky Method formulated as:

$$\mathrm{Sim}(X, Y) = \frac{2|X \cap Y|}{|X| + |Y|} \qquad (6)$$

By adding weight of Tversky-Method, the equation can be writen as :

$$\mathrm{Sim}(X, Y) = \frac{2\alpha(\#SAME(X, Y))}{2\alpha(\#SAME(X, Y)) + \beta(\#DIFFER(X, Y))} \qquad (7)$$

VI. METHODOLOGY

The implementation of Case-based Reasoning method to diagnose mood [affective] disorder consists of three parts: contruction of case base, input text processing and case retrieval process, as shown in Figure-1:
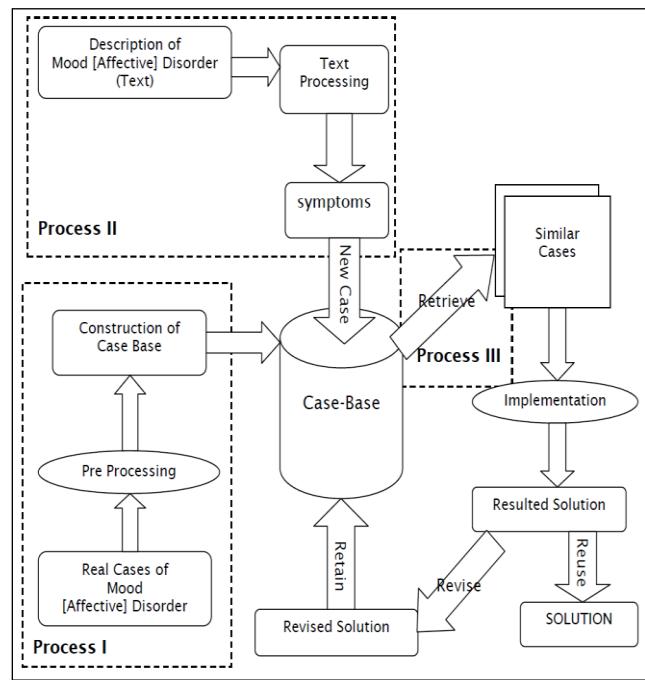
Fig. 1.   The proposed CBR implementation method

Contruction of case base is done by real life cases from various sources including the internet. The case base is then acquired as shown in Table-1:

TABLE I.   CASE BASIS

No	Codes	Name of Mood Disorder	Symptoms Codes
1	F30.0	Hipomania	G13, G14, G15, G16, G25, G26, G27, G28
2	F30.0	Hipomania	G13, G14, G17, G19, G25, G26, G27, G28, G46
3	F32.1	Depression II	G36, G37, G38, G39, G40, G41, G42, G43, G44, G45, G46
4	F32.0	Depression I	G36, G37, G39, G44, G53
5	F32.0	Depression I	G36, G38, G41, G44, G53
6	F32.0	Depression I	G37, G39, G41, G42, G44, G45, G46
7	F32.0	Depression I	G35, G36, G37, G38, G39, G41, G42, G43, G44
8	F32.1	Depression II	G36, G37, G38, G40, G41, G42, G44, G45, G46, G47, G48
9	F32.1	Depression II	G35, G37, G38, G39, G40, G41, G43, G44, G46, G47, G50, G53
10	F31.1	Bipolar II	G13, G14, G15, G17, G21, G24, G25, G26, G27, G28, G36, G46, G49, G52
11	F31.1	Bipolar II	G13, G14, G15, G17, G21, G24, G25, G26, G27, G28, G36, G46, G48, G52
12	F31.0	Bipolar I	G13, G17, G25, G27, G37, G38, G39, G40, G41, G42, G44, G48, G52
13	F31.0	Bipolar I	G13, G14, G17, G26, G30, G36, G38, G39, G40, G44, G46, G52
14	F30.0	Hipomania	G13, G14, G15, G17, G18, G19, G21

The explanation meaning of the symptoms codes are shown in Table -2.

TABLE II.   THE NAMES OF SYMPTOMS CODES

Id	Name of symptom
G13	increased mood
G14	increased energy and activity
G15	increased sociability, talkativeness and over familiarity
G16	increased sexual energy
G17	decreased need for sleep
G18	concentration and attention maybe impaired
G19	diminished the ability to settle down to work or to relaxation and leisure
G21	joviality
G23	easily distracted attention
G24	increased motoric activity
G25	talk too much
G26	self-esteem is inflated
G27	grandiose ideas
G28	over-optimistic ideas
G36	deminished energy and activity
G37	depressed mood
G38	loss of interest and enjoyment
G39	reduced concentration and attention
G40	reduced self-esteem and self-confidence
G41	idea of guilt and useless
G42	pessimistic
G43	idea of acts of self-harm
G44	disturbed sleep
G45	diminished appetite
G46	shows considerable distress
G47	loss of self-esteem
G48	attempted suicide
G52	decreased mood
G53	tiredness

Input text processing follow the steps above: tokenization, deletion of stop words, synonym search and replacement, N-gram configuration and symptoms diagnosis. Case retrieval is conducted by selecting a case from case base with the highest of case similarity degree. We implemented 3 methods to calculate the case similarity degree: Our Modified-Tversky, the original Tversky and Jaccard methods.

VII. RESULTS AND DISCUSSION

During text processing, testing is conducted through comparison of the number of symptoms used as the foundation of the input text configuration with those produced by text processing. The performance value is then formulated as:

$$P = \frac{NS}{NB} \times 100\% \qquad (8)$$

Where:

P = Performance

NS = The number of same symptoms obtained from text processing

NB = The number of symptoms in the text (ground truth)

In the test conducted, text processing performance is shown in Table-3.

TABLE III.   TEXT PROCESSING PERFORMANCE

No	Symptoms in the text (ground truth)	NB	Symptoms obtained from text processing	NS	P(%)
1	G36, G38, G39, G44, G53	5	G36, G38, G39, G44, G53	5	100
2	G36, G37, G39, G42, G53	5	G36, G37, G39, G42, G53	5	100
3	G13, G14, G16, G17, G18, G20	6	G13, G14, G16, G17, G18, G20	6	100
4	G36, G37, G38, G44	4	G36, G37, G38, G44	4	100
5	G13, G14, G15, G17, G18, G19, G20, G25	8	G13, G14, G15, G17, G18, G19, G20	7	87,5
6	G13, G14, G26, G27, G28, G36, G37, G38, G42, G43, G52	11	G13, G14, G27, G36, G37, G38, G42, G43, G48, G52	9	81,8
7	G13, G14, G16, G17, G18, G36, G46, G47, G48, G52, G53	11	G13, G14, G16, G17, G36, G43, G46, G48, G52, G53	9	81,8
8	G36, G37, G38, G39, G40, G41, G42, G46, G47, G48, G53	11	G37, G38, G39, G41, G43 G46, G47, G48, G53	8	72,7
9	G37, G38, G39, G42, G44, G53	6	G37, G38, G39, G44, G53	5	83,3
10	G36, G37, G38, G39, G43, G44, G53	7	G36, G37, G38, G39, G44, G53	6	85,7
Average Performance of Text Processing					**89,3**

Based on Table-2, the average performance of text processing of the test data is 89.3%. In several tests show that the performance of text processing does not reach 100 %, it indicates that the text processing algorithms in this study cannot always produce the correct result due to different interpretation of words, therefore the algorithm can be developed in order to improve performance.

During case retrieval, experiments are conducted by evaluating the correspondence of the diagnosis given by experts with the one produced by the CBR system and the case similarities degree generated. The entire results of the case retrieval experiment of 10 new problems are shown in Table-4:

TABLE IV.   CASE RETRIEVAL TEST RESULTS

No.	Expert Diagnose	CBR Diagnose	Case Similarity degree (%)		
			Modified-Tversky	Jaccard	Tversky
1	F32.0	F32.0	88,89	66,67	80,00
2	F32.0	F32.0	88,89	66,67	80,00
3	F30.0	F30.0	44,44	44,44	28,57
4	F32.0	F32.0	36,44	36,44	22,22
5	F30.0	F30.0	83,33	55,56	71,43
6	F31.0	F31.0	43.75	43,75	28,75
7	F31.1	F31.1	41,18	41,18	25,93
8	F32.1	F32.1	86,49	61,54	76,19
9	F32.0	F32.0	88,89	66,67	80,00
10	F32.0	F32.0	95,24	83,33	90,91

The table shows that out of the three methods used in calculating of case similarity degree, the Modified-Tversky Method produces the best result. The statement is based on the all results of the test, as the suggested Modified-Tversky Method consistently generates better or at least equal outcome compared to other methods. This could be used as a refference in determining the method to calculate case similarity degree in future CBR researches. Based on Tebel-4 is also known that the diagnosis is generated by the CBR system in accordance with the diagnosis given by experts.

VIII. CONCLUSION

In compliance with the test results and analysis carried out in this research, conclusions can be drawn as such: The modified-Tversky method outperforms the Jaccars and Tversky methods. In all the tests conducted, results of case similarity measures using the Modified-Tversky method is greater than or equal to the calculations performed using the Jaccard dan Tversky methods. The test results also provide an average level of performance in processing text input is 89.3%. However, in future work can be developed text processing algorithms in order to improve the performance of text processing. Cases on the case-base should be added so that the system can handle the problems of mood disorders. Therefore, it takes a lot of supporting data relating to the case of mood disorders.

REFFERENCES

[1] A. Aamold, *"Case-based reasoning: Foundation issues". AICOM* **7,** pp 39-59, 1994

[2] A. Aamold and E. Plaza, "Case-based Reasoning: foundation issues, methodological variation and System approach", *AI Communication 7(1), pp. 39-59,* 1994

[3] A. Nasir and A. Muhith, "The Fundamental of Psychiatric Nursing: Introduction and Theory", Salemba Medika, Jakarta, 2010

[4] M. Denis, and A. Jasmin, "Applying Case-based reasoning for mobile support in diagnosing infective diseases". International Conference on Signal Processing Systems, IEEE Computer Society, pp 779-783, 2009

[5] B. Chakraborty, I. Srinivas, P. Sood, V. Nabhi, D. Ghosh, " Case Based Reasoning Methodology for Diagnosis of Swine Flu", IEEE GCC Conference and Exhibition, 19-22 Februari 2011, Dubai, United Arab Emirates, pp. 132-135, 2011

[6] P. P. S. Tomar, R. Singh, P. K. Saxena, and J. Sharma, "Case Based Medical Diagnosis of Occupational Chronic Lung Diseases From Their Symptoms and Signs", International Journal of Biometrics and Bioinformatics (IJBB), Volume (5) : Issue (4), pp. 216-224, 2011

[7] S. Pant, and S. R. Joshi, "Case-Based Reasoning In Neurological Domain", IEEE 978-1-4673-2590-5/12, 2012

[8] K. Ghorai, S. Saha, A. Bakshi, A. Mahanti, and P. Ray, "An mHealth Recommender for Smoking Cessation using Case Based Reasoning", 46th Hawaii International Conference on System Sciences, pp. 2695-2704, 2013

[9] B. J. Sadock and V. A. Sadock, "Mood disorder" In : *Kaplan & Sadock's Synopsis of Psychiatry: Behavioral Sciences/Clinical Psychiatry, 10th Edition*. Wolters Kluwer/Phiadelphia. Lippincott Williams & Wilkins, 2007

[10] E. Dalami, "Nursing Clients with Mental Disorder", Trans Info Media, Jakarta, 2009

[11] E. Vieta, "Managing Bipolar Disorder in Clinical Practice", second edition, London UK. Current Medicine Group Ltd., 2009

[12] S. Ferilli, F. Esposito, and D. Grieco, "Automatic Learning of Linguistic Resources for Stopword Removal and Stemming from Text", *Procedia Computer Science*, 38, 116–123, 2014

[13] O. Serban, G. Castellano, A. Pauchet, A. Rogozan, and J. P. Pecuchet, "Fusion of Smile, Valence and NGram Features for Automatic Affect Detection", *Humaine Association Conference on Affective Computing and Intelligent Interaction,* 2013

[14] G. Kowalski, "Information Retrieval Architechture and Algorithm", Springer, New York, USA. E-Book (e-ISBN 978-1-4419-7716-8), 2011

[15] S. K. Pal, and S. C. K. Shiu, "Foundation of Soft Case Based Reasoning", John Wiley & Sons, New Jersey, 2004

Instruments and Criteria for Research and Analysis of the Internet Visibility of Bulgarian Judicial Institutions WEB-Space*

Nayden Valkov Nenkov
Faculty of Mathematics and Informatics
University of Shumen "Episkop Konstantin Preslavsky"
Shumen, Bulgaria

Mariana Mateeva Petrova
Faculty of Mathematics and Informatics
St. Cyril and St. Methodius University of Veliko Turnovo,
Bulgaria

Abstract—**e-Justice has been under discussion at European level since 2007. The article describes some tools and displays objective criteria for evaluating the WEB-pages of judicial institutions in Bulgaria. A methodology is offered in order to improve the organization and functioning of the judicial institutions. It is used to conduct experimental tests for analysis and assessment of the main characteristics of the Bulgaria courts' WEB-sites. The results provide grounds for findings and recommendations leading to improved communication and the presence of these institutions in the WEB**.

Keywords—judicial institution; WEB-page; SEO (search engine optimization); evaluation criteria; court

I. INTRODUCTION

The evaluation of the judicial WEB-sites is an important task in the context of the radical reform made in this area. This evaluation must be consistent with the overall vision and the project to build an e-government with the EC requirements and the standards which exist for e-administration and e-services to the population in Bulgaria [1, 3].

On 18 December 2008 The European Parliament adopted a Resolution on e-Justice, on 22 October 2013 it adopted a Resolution on e-Justice calling for the use of electronic applications, the electronic provision of documents, the use of videoconferencing and the interconnection of judicial and administrative registers to be increased, in order to further reduce the cost of judicial and out-of-court proceedings [4, 7].

The existing European roadmap covers the objectives for the European projects in the field of e-Justice up until 2013. Some of the existing projects will only bear visible results after that period since the development of European-wide IT projects of preliminary groundwork.

Along with the many administrative, organizational, social and aesthetic requirements [6, 10, 11], there are also technical ones. They have been largely set in a number of tools to evaluate the WEB-content of the sites. The existence of a web-site is not enough. The questions, related to the Internet visibility of the web-site, are also of importance.

The official list of all courts is published on the website of the Supreme Judicial Council. Links to the websites of all courts are available on the website of the Supreme Cassation Court in the section "Useful links".

The first stage of the study was implemented in January 2013 between 07 and 14. The survey covered all courts by type: 7 Appellate courts; 28 District courts; 113 Regional courts; 5 Military courts; 28 Administrative courts and the Specialized Criminal Court [5, 6].

II. EXPOSITION

The subject of the study is to improve the presence of judicial institutions on the WEB in order to provide the necessary services citizens and the transparency of their activities. Part of the reviewed tools is used for SEO-optimization, but it is not the focus here and goes beyond the scope of issues discussed.

Before evaluating a WEB-site of an administrative unit of the judicial system, we should establish the criteria and their weight in the overall assessment. The analyzed sources [2, 3, 8, 12] offer various criteria that show different quantitative and qualitative characteristics of the sites.

There are numerous tools that facilitate both WEB-designers and experts in the creation of this type of software, as well as the experts and managers responsible for them.

Therefore are need to validate the WEB-sites and their codes according to the standard of WWW [2, 12] and evaluate to various characteristics such as site rating, and more.

In order to meet the set requirements and criteria for accessibility level, set by the European Commission about the websites of public administration, and also to meet the requirements of the current Internet technologies, the Web-sites of the institutions must adhere to the standards of WCAG 2.0 and the level of compliance "Double-A". Web sites of the institutions should cover the accessibility level Double-A according to the latest standards of the World Wide Web Consortium - Web Content Accessibility Guidelines 2.0 (WCAG 2.0) by the using best practices and techniques.

III. TOOLS

Here are discussed some of the most commonly used tools in practice, which give an idea of the types of tests and WEB-sites' inspection procedures.

A. The validator of W3C - Markup Validation Service

Markup Validation Service http://validator.w3.org/ - checks the validity of WEB-documents by using the scripting languages: HTML, XHTML, SMIL, MathML and checking whether the site carries out the ISO / IEC standard 15445: 2000 Information technology - Document description and processing languages - HyperText Markup Language (HTML) [2, 11]. For the validation a specific content such as RSS / Atom feeds or CSS styles, MobileOK content, or to find broken links is which there are other varieties of that validator are used for.

B. SEO-optimization Tool

"SEO-optimization Tool" [11, 12] also deserves attention, but only some of its functions can be used for free: check site ranking, loading speed and coding URL, while others like the automatic SEO analysis and analysis of external links are to be paid for.

C. Open Site Explorer Tool

The tool „Open Site Explorer"(fig.1) is powerful and multi-functional [9], gives an option for complex optimization. It allows to evaluate the rating of the domain, the WEB-site, the link metrics, the social metrics (not available in trial version), and the quantitative assessment of the sanctioned spam and inbound links to the site.
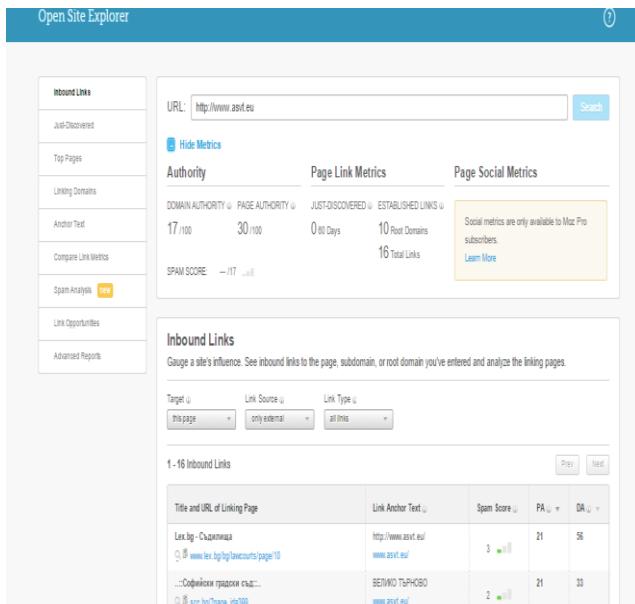
Fig. 1.   Tool for complex SEO-optimization and testing of WEB-sites

D. PINGDOM TOOLS

PINGDOM TOOLS provide some excellent possibilities for precise monitoring of WEB-sites (Fig. 2). Pingdom performs a global monitoring of WEB-sites and WEB-applications [8]. It has the following functions:

Uptime MONITORING – tests and verifies the presence of sites in the WEB-space every minute automatically from over 60 selected global locations

- REAL USER MONITORING – accumulates and stores valuable performance data of the WEB-site, based on

actual visits from users in order to improve its performance.

- TRANSACTION MONITORING - shows if important interactions and operations with the site such as registration, search or downloading files are slow or crashed.

- DevOps - integrates with other mostly cloud applications to correlate site data with given indicators in real-time, in order to improve productivity.

- RELIABLE – allows any problems encountered to be checked by a second opinion to achieve filtering of false alarms through this double check.

- ROOT CAUSE ANALYSIS - determines the causes of errors and interruptions in the WEB-site or server to solve problems and prevent their reoccurrence.
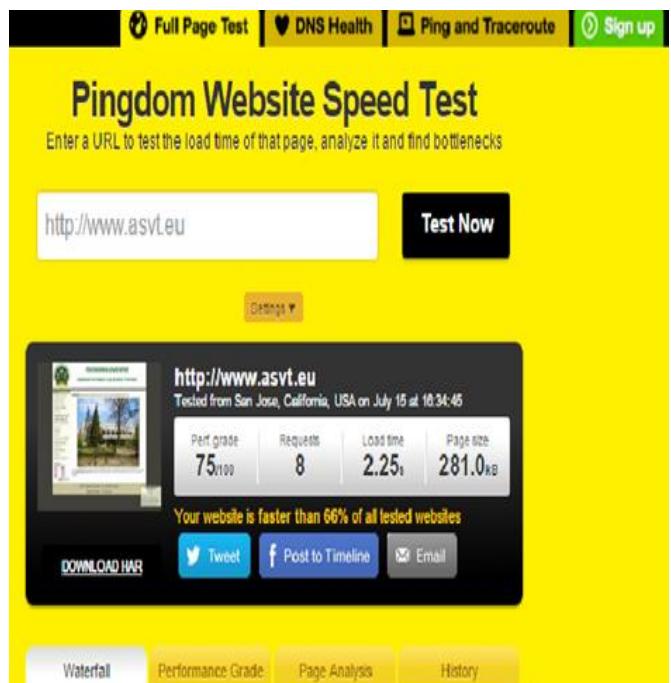
Fig. 2.   Pingdom tool for monitoring WEB-sites and WEB-applications

IV.   CRITERIA

The evaluation E of WEB-pages from sites of the judicial system can be defined by the multitude:

$$E = \{K_{ij}, O_j, S_j\} \qquad (1),$$

where $K_{ij} = V_{jk}$; $i = 1,..,m$; $j = 1,..,n$; $k = 1,...,b$; V_{jk} – numeric evaluations of the criteria, m – number of evaluation criteria (received by the tools for evaluating WEB-sites),

n — number of evaluated judicial institutions, b – extreme values of the scale of the evaluated values, complex criteria O_j and S_j have values in the interval + or –[0,…1].

The calculation of the criterion for evaluating the judicial WEB-sites is one of the most important stages in the process. You can define the following rules for calculation.

1) The value of the first criteria K1 is derived from the check with the validator described above (fig. 1) and is defined:

- If the site cannot be validated K_1 is not evaluated and is marked with **NO** in Table 1, part of which is shown below;

- If it is validated with errors, the derived value V_1 is recorded in the same table and $K_1 = V_1$ for the evaluated object;

- If there are no errors $V_1 = 0$ and so $K_1 = 0$.

2) The criterion reflecting a site's ranking in productivity K_2 is defined like that:

- If $K_2 = 0$ then K_2 is not evaluated and we do not record anything in Table 1 (leave an empty cell);

- Else the derived value V_2 is filled in the same table and $K_2 = V_2$ for the evaluated object.

The site is ranked, taking into account the results of tests passed until its conducting.

3) The number of requests necessary for loading the site V_3 define the criteria K_3

- If $K_3 = 0$ then K_3 is not evaluated and we do not record anything in Table 1 (leave an empty cell)

- Else the derived value V_3 is filled in the same table and $K_3 = V_3$ for the evaluated object.

This value describes the number of required elements of the site that need to be loaded for its proper operation.

4) Site loading time – V_4 defines the criterion K_4
It is defined in the following way:

- If $K_4 = 0$ then K_4 is not evaluated and we do not record anything in Table 1 (leave an empty cell)

- Else the derived value V_4 is filled in the same table and $K_4 = V_4$ for the evaluated object in seconds.

The largest and most authoritative company in this business GOOGLE ranks well a site only if it loads quickly. If the site is slow, it cannot optimize well.

The rating is good at loading speed from 0 to 1 sec, 2 to 3 seconds is average and the owners should work to improve it, and more than 4 seconds means that the owners must definitely optimize it.

5) Site total size - K_5
This criteria is defined like that:

- If $K_5=0$ then K_5 is not evaluated and we do not record anything in Table 1 (leave an empty cell)

- Else the derived value V_5 is filled in the same table and $K_5 = V_5$ for the evaluated object in seconds.

The size of the WEB-site should be optimal, depending on its purpose. The table is filled in with values in kilobytes (Kb). It is preferable the site to have a minimum size.

The results of the experiment conducted in May 2015 on 182 courts in Bulgaria are shown in Table 1.

TABLE I. PART OF THE EVALUATIONS OF THE JUDICIARY WEB-SITES IN BULGARIA

№	Name	WEB-site 2015	Valid. of WEB-sites (errors) V_1	Site rank by prod. (out of 100) V_2	Num. requests V_3	Load time (s) V_4	Site size (Kb) V_5
1	2	4	5	6	7	8	9
1	Burgas Court of Appeal	www.bgbas.org	21	87	29	0,829	131,4
2	Varna Court of Appeal	www.appealcourt-varna.org	1	85	20	1,39	250,5
5	Sofia Court of Appeal	acs.court-bg.org	no				
14	Administrative Court Burgas	http://www.admcourt-bs.org	19	82	29	1,97	250,5
…	…	…	…	…	…	…	…
182	Regional Court - Yambol	http://yambol.court-bg.org	no				

In order for the WEB-site to be evaluated, it is necessary to consider the impact of all criteria on its functionality. This is accomplished by making the following steps, which are used in the methodology [5, 6]:

A. Remove the results of experimental data beyond borders

It is believed they are due to errors in the reporting of the primary data obtained or other non-specific events during the experiment.

For each criteria, the mean square deviation is calculated and it is determined whether there are values out of range (- 3σ, + 3σ). If there are such values they are brought to value of the nearest border. WEB-sites that cannot be validated are excluded from calculations of further steps!

B. Normalization of criteria for evaluated objects - Web-sites of the courts

$$K_{ij} = \frac{v_{ij} - v_{javg}}{\sigma} * 100 \qquad (2)$$

Where K_{ij} – i criteria for the j site i= 1,…, m; j=1,….n.

Performed through transformation that takes into account the averages and deviations from them.

The obtained results are Table 2 where each of the rows contains a vector with values of the criteria K_1 to K_5 (column 2 to 6) for a WEB-site. The values which are negative are below average importance, and those with a positive sign are above average importance.

TABLE II. VALUES OF CRITERIA AND RANKING OF THE SITES OF THE JUDICIARY

№	K₁	K₂	K₃	K₄	K₅	Oᵢⱼ	Sᵢⱼ	R.
1.	2.	3.	4.	5.	6.	7.	8.	9.
160	-0,000963726	-0,3635488	-0,02933	-0,00128	-0,00102	0,760647	0,15212946	1
12	0,014442872	-0,360612219	-0,01798	-0,00142	-0,00086	0,729849	0,14596982	2
74	-0,005407937	0,360612219	0,018891	-0,00149	-0,00076	0,72707	0,14541391	3
7	0,007924696	0,360612219	-0,03784	-0,00082	-0,0012	0,697213	0,13944259	4
27	-0,001852569	0,323317632	-0,04351	-0,00138	-0,00076	0,695997	0,13919947	5
144	-0,002148849	0,360612219	-0,035	0,00155	0,000831	0,681209	0,13624183	6
57	-0,004222814	0,360612219	-0,02933	-0,00145	-0,00091	0,681092	0,13621841	7
…	…	…	…	…	…	…	…	…
104	0,003184	-0,001468	-0,000953	-0,000894	-0,000346	0,001239	0,000248	**137**

R. – rating.

C. The integrated evaluation of each site is determined by the expression:

$$O_i = \sum_{j=1}^{n} w_j \, v_{ij} \qquad (3)$$

where i =1,…m, j =1,…,n, w_j -weight coefficient indicating the importance of each criterion, v_{ij} - numeric value of criteria j for site i.

This evaluation O_{ij} weighs the different criteria in the final evaluation. In this case the weight of the first and the second criteria is $w_{1,2}$ =2, which means that they are basic and have a two times greater effect than the other three which are of weight $w_{3,4,5}$ =1. They are shown in column 7 of Table 2.

D. Complex evaluation of sites

$$S_i = \frac{\sum_{j=1}^{n} O_{ij}}{n} \qquad (4)$$

where i =1,…m, m-number of the evaluated sites (does not include non-validating sites), j =1,…,n, ,n=5, O_{ij} - integrated evaluation j for site i.

The complex evaluation of WEB-sites of the judicial system is calculated as the average of the evaluation of other criteria and their weighted influence. Thus the qualities of the development and functioning of the sites are considered. The results are in column 9 of Table 2.

V. DISCUSSION

The results show that 45 (24.73%) of the sites cannot be validated and are excluded from the evaluation. This leads to a violation of the standard and the urgent need to take action to resolve the issue.

The remaining 137 sites are validated with different number of errors in the code, adversely affecting their quality. There are 16 sites in which no errors were made and complied with standard WWW [2, 12].

The integrated O_i and the complex evaluation S_i are illustrated in Fig. 3.
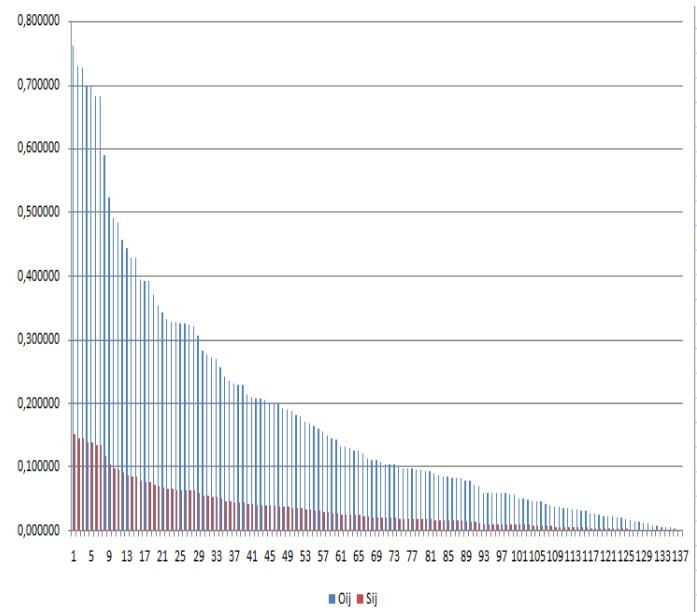
Fig. 3. Integrated and comprehensive assessment of websites

VI. CONCLUSION

The existing WEB-pages of the courts are evaluated by appropriately selected criteria, tools and methodology. The proposed conclusions and recommendations were obtained after analyzing the experimentally determined values of several criteria. They cover the important features of this type of communication and their visual expression in the WEB-space.

A large number (45) of the pages of judicial institutions are not validated and cannot be evaluated. They need to be adjusted and adapted to the standard for validating the content.

The remaining (137) WEB-pages have a large number of errors, which are subject to correction and improvement to reach a good level of maturity. This will ensure better results in the service of citizens and employees who work for these institutions.

REFERENCES

[1] G. Dimitrov, S. Manolov , L. Blagoev and A. Kuyumdzhieva, "State of the E-government in Bulgaria", Analysis, Law and Internet Foundation, Sofia, pp. 34-56, 2006.

[2] E. Castro, "HTML, XHTML & CSS", Visual Quickstart Guides, Sixth Edition, Peachpit Press, pp. 345-346, 2007.

[3] M. Petrova, "Informatization of public in Bulgaria", pp. 24-47, FABER, Veliko Tarnovo, 2014.

[4] M. Petrova and G. Dimitrov, "E-justice - the guarantee of an effective judicial system. Initiatives in Bulgaria", REVISTA NAŢIONALĂ DE DREPT (Publicaţie periodică ştiinţifico-practică), Universitatea de Stat

din Moldova, Chisinau, Moldova, nr.10-11 (133-134), pp. 169-173, 2011.

[5] M. Petrova, "Internet-presence and internet-exposure of the courts in Bulgaria", VI International Scientific Conference "Innovations in technology and education", KuzGTU, Belovo, May, 2013, v. 2, pp.159-165.

[6] M. Petrova, "Research of web-sites in the district courts of Bulgaria regulatory compliance", VI International Scientific Conference "Innovations in technology and education", KuzGTU, Belovo, May, 2013, v.2, pp. 159-165.

[7] Official Journal of the European Union, C 182, pp 2-13, Volume 57, June, 2014.

[8] "Optimize your Pingdom alerts", PINGDOM tutorial Tools, http://royal.pingdom.com/tag/tutorial/ Retrieved, July, 2015

[9] R. Fishkin and Moz Staff , "The beginer's Guide to SEO", http://d2eeipcrcdle6.cloudfront.net/guides/M-The-Beginners-Guide-To-SEO.pdf, Retrieved, August, 2015.

[10] M. Stefanova, T. Stefanov and O. Asenov, "Access to E-government' Services through Vein-code Biometric Identification", 7th Iberian Conference on Information Systems and Technologies, Madrid, Spain, June 2012, Vol. II, pp.174-176.

[11] Stefanov, T. "Methods for Assessing Information Sites", XLVII International Scientific Conference on Information, Communication and Energy Systems and Technologies ICEST'12, Bulgaria, Veliko Tarnovo, June 2012, Vol.2, pp. 455 – 458.

[12] Web Content Accessibility Guidelines (WCAG) Overview. World Wide Web Consortium, Retrieved, April, 2009.

A Directional Audible Sound System using Ultrasonic Transducers

Wen-Kung Tseng

Graduate Institute of Vehicle Engineering
National Changhua University of Education
Changhua City, Taiwan

Abstract—In general the audible sound has the characteristics of spreading, however the ultrasound is directional. This study used amplitude-modulating technique for an array of 8 ultrasonic transducers to produce directional audible sound beam. In this study sound field distribution for the directional audible sound beam has been investigated. The effect of different weightings varied with different frequency for the transducers on the directivity of the sound beam has also been evaluated. An H_∞ optimization method was used to calculate the optimal weightings of the transducers for better directivity of the sound beam. Different optimal weightings also added to the carrier and sideband frequencies to control the difference frequency's beam width and side lobe amplitude. The results showed that the beam width can be controlled and good directivity of the sound beam can be obtained by using the H_∞ optimization method.

Keywords—ultrasound; amplitude-modulating; directional audible sound beam; weightings; H_∞ optimization method

I.   INTRODUCTION

Generally, the audible sound frequency is the range from 20 Hz to 20 kHz; however, ultrasound is sound pressure with a frequency greater than the upper limit of human hearing i.e. 20 kHz as shown in Fig. 1. Recently the highly directional audible sound has been investigated for a few years. The audible sound has the characteristics of spreading, however the ultrasound is directional.

In the pass decades, the performance in the ultrasound systems and their beamforming has been studied. Beamforming is the concept of forming directional beams. Previous study [1] has discussed that two plane waves of different ultrasonic frequencies could generate the directional audible sound due to acoustical nonlinearity. There are mainly two new waves, one of which has a frequency equal to the decrease of the original two frequencies and the other equal to the difference frequency.

New ultrasonic waves whose frequencies correspond to the decrease and difference of the two ultrasonic signals will be produced. The nonlinear interaction of ultrasonic sound waves in air will produce this phenomenon. For instance, if there are two ultrasonic signals in the air at closely frequencies f_0 and f_1 as shown in Fig. 2, they will be transformed into $2f_0$, $2f_1$, $f_1 \pm f_0$ and other higher order harmonics in the signal [2]. The new components of $2f_0$, $2f_1$ and $f_1 + f_0$ in the air will be strongly attenuated rapidly with increasing distance from the transducer. However, the remaining frequency $f_1 - f_0$ is decay slowly with increasing distance from the transducer because of the relatively low absorption.

For simplicity, the ultrasonic transducer is fed with two ultrasonic signals f_0 at 40 kHz and f_1 at 41k Hz, then the new modulation frequency is 1 kHz ($f_1 - f_0$). The new frequency component of 1 kHz has lower absorption than other high-frequency terms. For this reason, this study will not discuss the new high-frequency terms. Instead, it will focus on and discuss the frequency subtraction component $f_1 - f_0$ of new frequency components.

Traditional in-car communication gadgets, such as cell phones or radios, generally adopt traditional loudspeakers to broadcast. This has several weaknesses. For instance, people in the car can all hear the sound. This makes it impossible to maintain privacy. Besides, people feel bothered and thus the ride quality would not be so pleasant. If cars are equipped with directional loudspeakers, each passenger can hear the different music or information. Thus, people would not feel bothered. Before directional loudspeakers are applied to vehicles, it is necessary to do through research on audible sound beams. Most of efforts were devoted to the preprocessing methods [3] and speaker design [4] for improving the system performance of the directional sound beam. On the other hand, several model equations have been presented to describe the propagation of finite-amplitude sound beams from the parametric array, which has been reviewed in Ref. [5]. More works were refer to the directional audible sound by using the parametric array [6, 7]. Yoneyama used an array of transducers to demodulate the broadband sound signals with reasonable loudness, and called the audio spotlight [5]. However, the approaches of beamforming require complex mathematics equations. As an alternative approach, the ultrasonic field is presented to a newly numerical computation [8, 9]. Also J. Yang. Et. [2] presented an algorithm to discuss the weighted parametric array.

Audible   Ultrasound

Fig. 1.   The range of ultrasound

There has been little work done on the beam width control in directional loudspeakers. Without the beam width control, the directivity of the sound beams is fixed, and it cannot meet the various needs while applying the directional loudspeakers to vehicles. In order to find a way to better control the directivity of the sound beams, papers concentrated on this issue have been closely reviewed so far, and the Chebyshev method has proven to be the only effective method on this issue [2, 8, 9].

However, this paper discusses the theoretical simulation controlling the directivity of the sound beams using the uniform linear array (ULA) composed of eight transducers. An H_∞ optimization method is used to investigate the weighting distribution of uniform linear array, and the influence on the spreading angle of the sound beam. The method proposed in the study can improve the performance of the directional audible sound for all frequencies. The optimal weighting values of the transducers corresponding to specific sound beam spreading angle can be used to control the beam width and the amplitude of the side lobe.
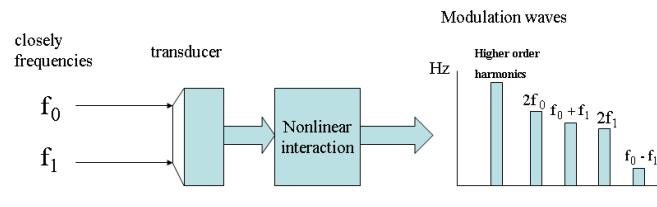

Fig. 2. Nonlinear phenomenon in the air

II. DESIGN OF DIRECTIONAL AUDIBLE SOUND SYSTMES

In this section the formulation for designing directional audible sound systems using an H_∞ control method is presented. The directional audible sound can be expressed by the Khokhlov–Zabolotskaya–Kuznetsov (KZK) equation which accurately describes the diffraction, absorption, and nonlinearity of ultrasound in a parametric array as follows [10].

$$\frac{\partial^2 p}{\partial z \partial \tau} = \frac{c_0}{2}\nabla_\perp^2 p + \frac{\delta}{2c_0^3}\frac{\partial^3 p}{\partial \tau^3} + \frac{\beta}{2\rho_0 c_0^3}\frac{\partial^2 p^2}{\partial z^2},\tag{1}$$

where

p = acoustic pressure
z = coordinate along the axis of the beam propagation direction
τ = retarded time
c_0 = small signal sound speed
ρ_0 = ambient density
δ = sound diffusivity
β = coefficient of nonlinearity
$\nabla_\perp^2$ = transverse Laplacian operator

Because of this successive approximations, a quasi-linear solution of the form $p = p_1 + p_2$ is assumed. Therefore p_1 is the linear solution of (1) for the primary pressure at frequency ω and p_2 is a small correction to p_1 at the second-harmonic frequency 2ω.

The definition becomes:

$$\mathbf{p_1}(\mathbf{r},\mathbf{z},\tau) = \frac{1}{2\mathbf{j}}[\mathbf{q_{1a}}(\mathbf{r},\mathbf{z})\mathbf{e}^{\mathbf{j}\omega_a\tau}$$
$$+ \mathbf{q_{1b}}(\mathbf{r},\mathbf{z})\mathbf{e}^{\mathbf{j}\omega_b\tau}] + c.c.,\tag{2}$$

$$\mathbf{p_2}(\mathbf{r},\mathbf{z},\tau) = \frac{1}{2\mathbf{j}}[\mathbf{q_{2a}}(\mathbf{r},\mathbf{z})\mathbf{e}^{\mathbf{j}2\omega_a\tau} + \mathbf{q_{2b}}(\mathbf{r},\mathbf{z})\mathbf{e}^{\mathbf{j}2\omega_b\tau}$$
$$+ \mathbf{q_+}(\mathbf{r},\mathbf{z})\mathbf{e}^{\mathbf{j}\omega_+\tau} + \mathbf{q_-}(\mathbf{r},\mathbf{z})\mathbf{e}^{\mathbf{j}\omega_-\tau}] + c.c.,\tag{3}$$

Then q_1 and q_2 are the complex pressure amplitudes, *c.c.* denotes the complex conjugate of preceding terms.

q_1 can be obtained from a homogeneous equation as:

$$\frac{\partial q_1}{\partial z} + \frac{i}{2k}\nabla_\perp^2 q_1 + \alpha_1 q_1 = 0\tag{4}$$

Then an inhomogeneous equation for q_2 is presented as:

$$\frac{\partial q_2}{\partial z} + \frac{i}{4k}\nabla_\perp^2 q_2 + \alpha_2 q_2 = \left(\frac{\beta k}{2\rho_0 c_0^2}\right)q_1^2\tag{5}$$

Where $k=\omega/c$ becomes the wave number, whereas $\alpha_n=\delta n^2\omega/2c^3$ is the thermos viscous attenuation coefficient at frequency $n\omega$. For a parametric speaker, we are only interested in the audible sound beam at difference frequency. Assume that the sound beam is caused to be at difference frequency $\omega_- = \omega_a -\omega_b$ ($\omega_a>\omega_b$), then ω_a and ω_b become the two primary frequencies. The result of the complex pressure amplitude q_- is:

$$q_-(r',z') = -\frac{\pi\beta k_-}{\rho_0 c_0^2}\int_0^z\int_0^\infty q_{1a}(r',z')\,q_{1b}^*(r',z')\,G_-(r,z|r',z')\,r'dr'dz'\tag{6}$$

Thus $k_- = \omega_-/c$, q_{1a} q_{1b} are the complex pressure amplitudes for frequencies ω_a and ω_b, relatively, G-(r, z|r

,

z

)is the Green's function presented as:

$$G_-(r,z|r',z') = \frac{ik_-}{2\pi(z-z')}J_0\left(\frac{k_-rr'}{z-z'}\right)\exp\left[-\alpha_-(z-z') - \frac{ik_-(r^2+r'^2)}{2(z-z')}\right]\tag{7}$$

Then $\alpha_- = \delta\omega_-^2/2c^3$, and J_0 become the zeroth-order Bessel function. Being simple, we consider the sound beams produced by a primary source with Gaussian amplitude shading. While the complex pressure amplitude $q_1(r, 0)$ at primary frequency can be determined as:

$$q_1(r,0) = p_0\exp\left[-\left(\frac{r}{a}\right)^2\right]\tag{8}$$

On the other hand p_0 is the peak source pressure and a is the effective source radius.

Then, the linear solution can be deduced as:

$$q_1(r,z) = \frac{p_0 e^{-\alpha_1 z}}{1-iz/z_0}\exp\left[-\frac{(r/a)^2}{1-iz/z_0}\right]\tag{9}$$

Where $Z_0 = \frac{1}{2}ka^2$. The far-field solution of the directivity is

given by

$$D_1(k,\theta) = \exp\left[-\frac{1}{4}(ka)^2 \tan^2\theta\right] \qquad (10)$$

Assume that we only considered one far-field, according to a bi-frequency Gaussian source, the far-field directivity of different frequency is described by the product of the directivity function, i.e.:

$$D_-(\theta) = D_{1a}(\theta)D_{1b}(\theta) \qquad (11)$$

Thus, for a bi-frequency Gaussian source the far-field directivity of the difference frequency is described by the product of the directivity functions of the primary waves.

Assume that a group of M ultrasonic transducers is arranged in a uniform linear array (ULA) with an inter element spacing of d as shown in Fig. 3. An observation point is set in the far-field of the array at an angle, θ with respect to the normal of the transducer array aperture. If each transducer is weighted with a weighting, ω_m for m=0, 1, 2, . . ., M−1, the array response function [11] can be derived as:

$$H(\omega\tau) = \frac{1}{M}\sum_{m=0}^{M-1} w_m e^{im\omega\tau} \qquad (12)$$

Where,

$\tau = \text{d}/c\sin\theta_0$ is the time delay.

ω_m , m = 0,1,2,3…..M-1 is the weighting for each transducer

θ is the angel with respect to the axis of the beam.

In selecting proper weightings, the side lobes level can be made suitable at the expense of the beam width of the main lobe. From (12), it showed that the maximum of the main lobe exists on the broadside of the ULA ($\theta = 0$). However, the maximum of the main lobe can be changed by adding a phase shift or delay to each transducer. If the ULA is to be steered in the direction θ_0, time delay ($m\tau_0$) has to be added to mth transducer before transmitting the signal into the air. The time delay τ_0 can be calculated as $\tau = (\text{d}/c)\times\sin\theta_0$, and the array response of the delay-and-sum beamforming becomes:

$$H(\omega\tau) = \frac{1}{M}\sum_{m=0}^{M-1} w_m e^{-im\omega(\sin\theta_0-\sin\theta)d/c_0} \qquad (13)$$

Then, the far-field directivity of the weighted primary sources array for frequency ω_a, $D_{1a}(\theta)$ can be appeared:

$$D_{1a}(\theta) = D_1(k_a,\theta)H(k_a,\theta) \qquad (14)$$

When $D_1(k_a, \theta)$ is the aperture directivity shown in (10) for frequency ω_a, and the far-field array response $H(k_a, \theta)$ is indicated in (12) with w_{am} and ω_a instead of w_m and ω. Similarly, the far-field directivity for primary frequency ω_b, $D_{1b}(\theta)$ can be shown as:

$$D_{1b}(\theta) = D_1(k_b,\theta)H(k_b,\theta) \qquad (15)$$

$D_1(k_b, \theta)$ and $H(k_b, \theta)$ are written as (10) and (12) for frequency ω_b with w_{bm} instead of w_{am}. Therefore, the beam pattern of the audible frequency is produced by substituting (12) and (13) into (14):

$$D_-(\theta) = D_1(k_a,\theta)H(k_a,\theta)D_1(k_b,\theta)H(k_b,\theta) \qquad (16)$$

Thus, by substituting (10),(13) into (16) ,the directivity of far-field difference frequency equation can be written as:

$$D_-(\theta) = \exp[-\frac{1}{4}(k_a*a)^2\tan^2\theta]*\frac{1}{M}\sum_{m=0}^{M-1}\omega_m e^{-jm\omega(\sin\theta_0-\sin\theta)d/c}*$$

$$\exp[-\frac{1}{4}(k_b*a)^2\tan^2\theta]*\frac{1}{M}\sum_{m=0}^{M-1}\omega_m e^{-jm\omega(\sin\theta_0-\sin\theta)d/c} \qquad (17)$$
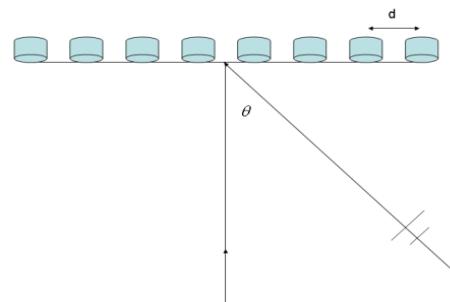
Fig. 3. Single array of M ultrasonic transducers

In this work the H_∞ optimization method is used to control the directivity of ultrasonic transducers. The design formulation can be written as:

Minimize σ
Subject to

$$\left\|D_-(\theta_{\text{sidelobe1}})\right\|_\infty < \sigma \qquad -40<\theta<-1/2\Delta$$

$$\left\|D_-(\theta_{\text{sidelobe2}})\right\|_\infty < \sigma \qquad 1/2\Delta<\theta<40$$

$$\left\|D_-(\theta_{\text{mainlobe}})\right\|_\infty - \left\|D_-(\theta_{\text{sidelobe1}})\right\|_\infty > \varepsilon \qquad -1/2\Delta<\theta<1/2\Delta$$

$$\left\|D_-(\theta_{\text{mainlobe}})\right\|_\infty - \left\|D_-(\theta_{\text{sidelobe2}})\right\|_\infty > \varepsilon \qquad -1/2\Delta<\theta<1/2\Delta \qquad (18)$$

where

σ is the real number.

Δ is the beam width, and ε is the amplitude difference between the main lobe and side lobe.

Substituting (17) into (18) gets:

$$\exp[-\frac{1}{4}(k_a * a)^2 \tan^2\theta_{sidelobe1}] * \frac{1}{M}\sum_{m=0}^{M-1}w_a(f_a)e^{-jm\omega(\sin\theta_0 - \sin\theta_{sidelobe1})d/c} *$$

$$\exp[-\frac{1}{4}(k_b * a)^2 \tan^2\theta_{sidelobe1}] * \frac{1}{M}\sum_{m=0}^{M-1}w_b(f_b)e^{-jm\omega(\sin\theta_0 - \sin\theta_{sidelobe1})d/c} < \sigma$$

$-40<\theta<-1/2\Delta$

$$\exp[-\frac{1}{4}(k_a * a)^2 \tan^2\theta_{sidelobe2}] * \frac{1}{M}\sum_{m=0}^{M-1}w_a(f_a)e^{-jm\omega(\sin\theta_0 - \sin\theta_{sidelobe2})d/c} *$$

$$\exp[-\frac{1}{4}(k_b * a)^2 \tan^2_{sidelobe2}] * \frac{1}{M}\sum_{m=0}^{M-1}w_b(f_b)e^{-jm\omega(\sin\theta_0 - \sin\theta_{sidelobe2})d/c} < \sigma \qquad 1/2\Delta<\theta<40$$

$$\exp[-\frac{1}{4}(k_a * a)^2 \tan^2\theta_{mainlobe}] * \frac{1}{M}\sum_{m=0}^{M-1}w_a(f_a)e^{-jm\omega(\sin\theta_0 - \sin\theta_{mainlobe})d/c} *$$

$$\exp[-\frac{1}{4}(k_b * a)^2 \tan^2\theta_{mainlobe}] * \frac{1}{M}\sum_{m=0}^{M-1}w_b(f_b)e^{-jm\omega(\sin\theta_0 - \sin\theta_{mainlobe})d/c} -$$

$$\exp[-\frac{1}{4}(k_a * a)^2 \tan^2\theta_{sidelobe1}] * \frac{1}{M}\sum_{m=0}^{M-1}w_a(f_a)e^{-jm\omega(\sin\theta_0 - \sin\theta_{sidelobe1})d/c} *$$

$$\exp[-\frac{1}{4}(k_b * a)^2 \tan^2\theta_{sidelobe1}] * \frac{1}{M}\sum_{m=0}^{M-1}w_b(f_b)e^{-jm\omega(\sin\theta_0 - \sin\theta_{sidelobe1})d/c} > \varepsilon$$

$-1/2\Delta<\theta<1/2\Delta$

$$\exp[-\frac{1}{4}(k_a * a)^2 \tan^2\theta_{mainlobe}] * \frac{1}{M}\sum_{m=0}^{M-1}w_a(f_a)e^{-jm\omega(\sin\theta_0 - \sin\theta_{mainlobe})d/c} *$$

$$\exp[-\frac{1}{4}(k_b * a)^2 \tan^2\theta_{mainlobe}] * \frac{1}{M}\sum_{m=0}^{M-1}w_b(f_b)e^{-jm\omega(\sin\theta_0 - \sin\theta_{mainlobe})d/c} -$$

$$\exp[-\frac{1}{4}(k_a * a)^2 \tan^2\theta_{sidelobe2}] * \frac{1}{M}\sum_{m=0}^{M-1}w_a(f_a)e^{-jm\omega(\sin\theta_0 - \sin\theta_{sidelobe2})d/c} *$$

$$\exp[-\frac{1}{4}(k_b * a)^2 \tan^2\theta_{sidelobe2}] * \frac{1}{M}\sum_{m=0}^{M-1}w_b(f_b)e^{-jm\omega(\sin\theta_0 - \sin\theta_{sidelobe2})d/c} > \varepsilon$$

$-1/2\Delta<\theta<1/2\Delta$ (19)

The performance of optimization is according to the different concerns of the constraints. During the simulation, different constrains would lead to different levels of performances. We used optimization method to find the optimal weightings which varied with frequency. The constraints in (19) are not the only possible types of constrains. Commonly, the different types of constrains can results in different performance, i.e. the beam width and amplitude of the side lobe in this work, for example.

III. SIMULATION RESULTS

In this section the simulation results for the directivity of the audible sound beam created by using the H_∞ optimization method are presented, and then compared to those obtained by using Chebyshev weighting method [2]. In this study, the number of weightings is 16 for frequencies f_a and f_b as shown in Fig. 4. Therefore there are 16 design variables, i.e. $\{h_{a0}, h_{a1}, ..., h_{a7}\}\{h_{b0}, h_{b1}, ..., h_{b7}\}$,

The carrier frequency of the ultrasonic transducer array is set as 40 kHz, i.e. f_a = 40 kHz. The demodulated signal is at the frequency from 500 to 20,000 Hz with 500 Hz interval. A total of M = 8 ultrasonic transducer array is used with inter-element spacing, d = 9.7 mm. The effective source radius is set at a = 3.85 mm and the speed of sound c is 344 ms^{-1}. The weightings, h_{an} and h_{bn}, are calculated for difference frequency's beam width, $\theta_- = 20^0$, 40^0 and 60^0 using the proposed method.

Figs. 5, 6 and 7 show the difference frequency's directivity for $\theta_- = 20^0$, 40^0 and 60^0 respectively. Figs. 5(a), 6(a) and 7(a) are the difference frequency's directivity using Chebyshev weighting method [8], and Figs. 5(b), 6(b) and 7(b) are the difference frequency's directivity using the optimization method for weightings varied with frequency proposed in the paper. From the figures it can be seen that the amplitude in the side lobe using the proposed method is lower than that using Chebyshev weighting method. This is because the optimization method tried to find the optimal weightings which minimize the amplitude of the side lobe and subject to the amplitude difference between the main lobe and the side lobe. Therefore the optimization method proposed in this paper performs better than Chebyshev weighting method. As can be seen from the figures the beam width can also be controlled using the optimization method. This is because the difference frequency's directivity is the product of two primary frequency's directivities, its beam width always takes on the narrowest beam width of the two primary waves. It can obviously be seen that a constant beam width is achieved for all frequencies using the proposed method.

The highest side lobe amplitude with the proposed method gets attenuated more compared to the method with Chebyshev weighting. This is since the amplitude of the side lobe region is minimized through all the frequencies. Therefore the lower side lobe amplitude is obtained using the propose method.

IV. CONCLUSIONS

In this paper the H_∞ optimization method has been proposed for designing directional audible sound beam. The directional audible sound beam was generated by using a uniform linear array composed of eight ultrasonic transducers with different weightings varied with frequency. The performance of the beam width control using the proposed method has been evaluated. It can be seen that the proposed method could effectively control the beam width and the level of the side lobes for the audible sound beam. It is verified by the simulation results that the lower side lobes level could be obtained by using the proposed method. Therefore the proposed method could improve the system performance compared to that with the Chebyshev weighting method.

ACKNOWLEDGMENT

REFERENCES

[1] P. J. Westervelt, ''Parametric acoustic array'', Journal of Acoustical Society of America, Vol. 35, no. 4, 1963, pp.535-537.

[2] Yang Jun, W. S. Gan, K. S. Tan, Er M. H., ''Acoustic beamforming of a parametric speaker comprising ultrasonic transducers'', Sensors and Actuators, A 125: 2005, pp.91-99.

[3] H. O. Berktay, ''Possible exploitation of nonlinear acoustics in underwater transmitting applications'', Journal of Sound & Vibration, Vol. 2, no. 4, 1965, pp. 435-461.

[4] Y. Roh and C. Moon,. "Design and fabrication of an ultrasonic speaker with thickness mode piezoceramic transducers", Sens. Actuators A 99, 2002, pp. 321–326.

[5] M. Yoneyama, and J. Fujimoto, ''The audio spotlight: An application of nonliear interaction of sound waves to a new type of loudspeaker design'', Journal of Acoustical Society of America, Vol. 73, no. 5, 1983, pp. 1532-1536.

[6] F. J. Pompei, Parametric audio system, WO 01/52437 A1, 2001.

[7] M. E. Spencer, and J. J. Croft, Modulator Processing for a Parametric Speaker System, WO 01/15491 A1, 2001.

[8] W. S. Gan, Yang Jun, K. S. Tan, Er M. H., ''A digital beamsteerer for difference frequency in a parametric array'', IEEE transactions on audio, speech, and language processing, 14(3), 2006, pp. 1018-1025.

[9] K. S. Tan, W. Gan, S. J. Yang, and Er, M. H.. "Constant beamwidth beam-former for difference frequency in parametric array", in Proc. ICASSP , 2003, pp.361–364.

[10] M. F. Hamilton and D.T. Blackstock, Nonlinear Acoustics, Academic press, San Diego, 1998.   D. H. Johnson and D. E. Dudgeon, Array signal processing, Prentice Hall, New Jersey, 1993.
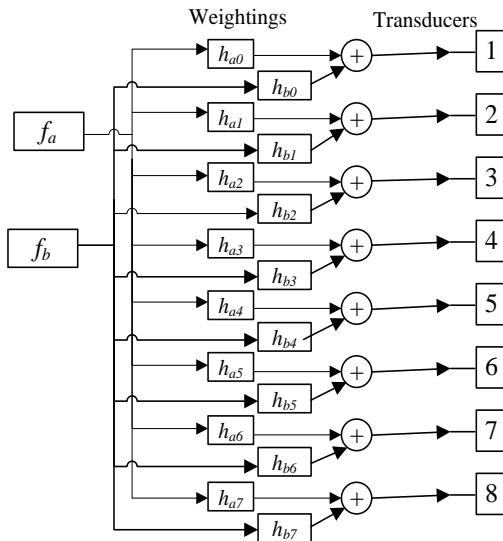
Fig. 4. Block diagram for beam width control systems with different weightings

(a)

(b)

Fig. 6. Difference frequency's directivity for $\theta_- = 40^0$. (a) Chebyshev weighting method. (b) Optimization method for weightings varied with frequency
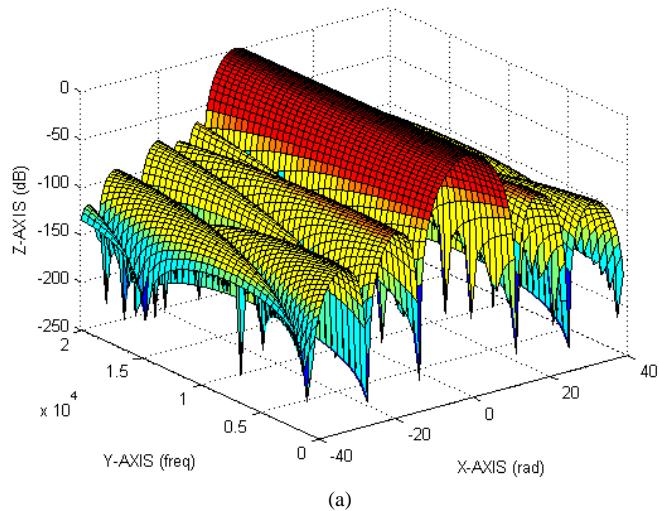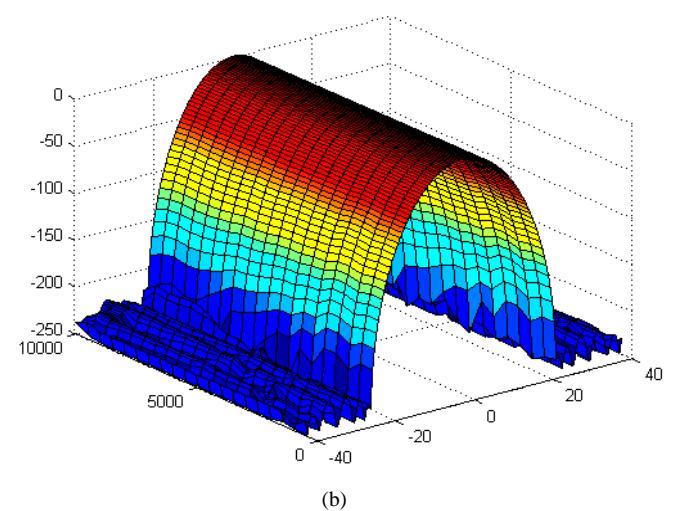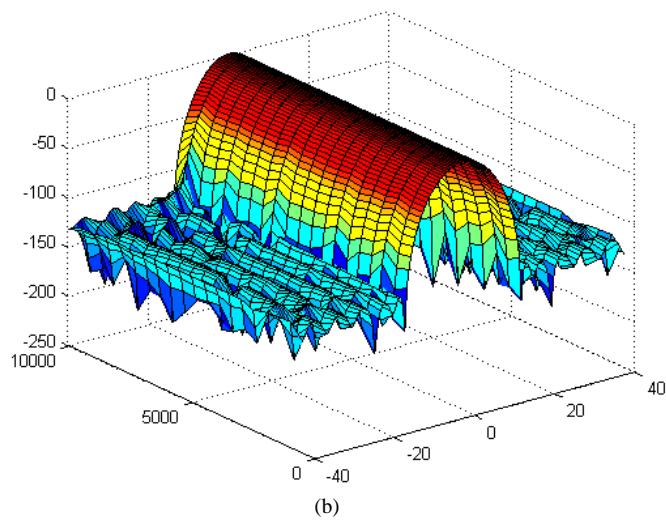
(b)

Fig. 5. Difference frequency's directivity for $\theta_- = 20^0$. (a) Chebyshev weighting method. (b) Optimization method for weightings varied with frequency

(a)

(a)

(b)

Fig. 7. Difference frequency's directivity for $\theta_- = 60^0$. (a) Chebyshev weighting method. (b) Optimization method for weightings varied with frequency

System for Human Detection in Image Based on Intel Galileo

Rastislav Eštók

Dept. of Computers and Informatics
FEI TU of Kosice
Kosice, Slovak Republic

Ondrej Kainz

Dept. of Computers and Informatics
FEI TU of Kosice
Kosice, Slovak Republic

Miroslav Michalko

Dept. of Computers and Informatics
FEI TU of Kosice
Kosice, Slovak Republic

František Jakab

Dept. of Computers and Informatics
FEI TU of Kosice
Kosice, Slovak Republic

Abstract—**The aim of this paper is a comparative analysis of methods for motion detection and human recognition in the image. Authors propose the own solution following the comparative analysis of current approaches. Then authors design and implement hardware and software solution for motion detection in the video with human recognition in the picture. The development board Intel Galileo serves as the basis for hardware implementation. Authors implement own software solution for motion detection and human recognition in the image, resulting in the evaluation of proposed implementation.**

Keywords—image processing; Intel Galileo; motion detection; object recognition

I. Introduction

Motion detection and objects recognition in the image is an active research being done as a part of computer science. The principal goal of intelligent systems for objects recognition and tracking is the use of these systems in various sectors of computer engineering, e.g. image processing, security, and robotics. People can focus on a specific object, and the aim of the research is to implement this ability in intelligent systems.

The object is in motion when it is compelled to change that state by force impressed on it. Detecting the motion is the object is done by [1]: sound, optical, vibration, geomagnetism, refection of transmitted energy and electromagnetic induction. Detection of motion by sound follows the principle that every object being in movement causes sound and detector can localize the source of sound in the area.

The most used methods for motion detection are optical methods compare frames from continuous video stream and detect moving objects. Video sequence source is in MJPEG and there are techniques to convert this stream into JPEG images. In this paper authors compare two frames images in bitmap image file which support RGB color model. Project consisted of both, hardware and software implementation. The first, utilize the Intel Galileo board and IP camera and the latter introduces and approach for detection of person directly by the proposed device. In the following sections, the well-known approaches in the area of detection are presented.

II. Motion Detection Methods in Video Sequence

There is a great number of the algorithms for tracking objects in video sequence, most of them uses comparison of one frame from video to the previous one. Three common methods are used for motion detection in video sequence [1]. These methods are background subtraction, optical flow and temporal differences. Systems for motion detection needs to handle a number of critical problems. The most common described in [2] are variations of the lighting conditions, small non-static movements such as tree branches in the wind, low image quality source making noise picture; movements in ghost regions in the image or sudden changes in the light conditions inside by presence of a light switch and outside by clouding. There is no system that would provide exact output and work without errors. The goal of every technique is to reach the best results without mistakes caused by described critical problems. It is recommended to combine two or more techniques to acquire better results.

A. Background Subtraction

There are a lot of algorithms for background subtraction methods and majority of them is based on principles described in [3] and shown on flow diagram in Fig. 1.
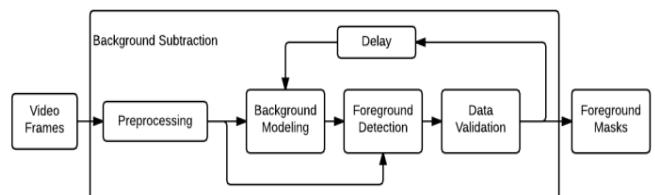
Fig. 1.   Flow diagram of a generic background subtraction algorithm [3]

Fig. 1 represents a simple flow diagram that describes generic algorithm for the background subtraction. It is composed of four main parts: preprocessing, background modeling, foreground detection and data validation. Preprocessing is a process for setting videos properties. Video from camera is captured in real-time in required format with

image processing. The video is divided to frames in this part of background subtraction process. The next part is background modeling. This is the main part of all process. There has been many researched towards the finding of robust background modeling techniques. The aim of these researches is described in [3] and it is to seek a balanced technique which is robust against environmental changes in background, but enough sensitive to identify all the moving object of interest. Foreground detection is part where are identified all pixels from image which are candidates for foreground pixels. The outputs of this part are objects in foreground. Subsequently there is a data validation part where candidates for foreground are identified and verified.

There are two different types of background modeling in background subtraction techniques: non-recursive and recursive techniques.

Non-recursive techniques use a buffer in a sliding-window which stores previous frame and estimates the background image based on temporal variations of each pixel in a buffer. These methods are adaptive, because they do not depend on history beyond those frames stored in the buffer. There is a large storage requirement depending on buffer size. In [3] the authors describe common non-recursive techniques for background modeling, i.e.: frame differencing, median filter, linear predictive filter and non-parametric model.

Recursive techniques do not use buffer for background estimation. They recursively updates background model in each input frame. Input frames from past could have an effect on new inputs. Recursive techniques do not need such storage. If an error occurs in recursive technique, it last more time to eliminate this error. Authors in [3] describe these recursive techniques for background modeling: approximated median filter, Kalman filter and mixture of Gaussians.

B. Optical flow

Method was described by Lucas and Kanade in [4] and based on this approaches there are three assumptions described in [5], these are: brightness constancy, temporal persistence and spatial coherence.

C. Temporal differences

This method is also called method of frame differences. Principles of this method are described by author in [6]. Method compares two frames and uses special techniques for electing referral object for motion detection. This technique is based templates and it is called template matching. Author in [1] describes two template matching techniques: static, used in background subtraction and dynamic template matching (DTM). This study uses frame differences method by comparing each of RGB components: red, green and blue. Method in this study compares all pixels from two frames and based on this detects the motion.

III. METHODS FOR FACE AND HUMAN RECOGNITION IN STATIC IMAGE

The aim of methods for face detection is to find out if there is a face in a static picture. In positive case the face is localized and system returns face location and parameters. Also in face recognition there are many factors that influence the results.

These factors are described in [2] and [7]. Face location may vary by camera position and angle of coverage. This can cause that faces are covered by other objects or are damaged. For example a nose may vary from any angle of coverage. Author in [8] described next factor. Presence or absence of structural components such as beards, mustaches or glasses which may or may not be present on face and there is a high variability of these components including shapes, color and size. Faces may vary by a person's facial expressions. Faces in picture may be occluded by other objects. There is also big possibility to damaging facing because of low image quality. Bed effect to face recognition is caused by lightning conditions that can vary very fast.

Author in [2] describes four common methods for face recognition in image: knowledge-based methods, feature invariant approaches, template matching methods and appearance-based methods.

A. Knowledge-based Methods

Knowledge-based methods use rules to define human faces properties. The rules describe relationships between parts of a face. These methods are used mainly for face localization in image. In general, it is simple to describe human face and relationships between each part of face. It is known that face is composed of one pair of eyes that are symmetric to each other, one nose, one mouth and other good known parts of face. Based on this information are created rules of relationship between each part. It is known that faces can be described with common rules. It is very important to set rules very effective. If relationships are described very exactly, there are a lot of mistakes in face recognition. On the other side, if rules are more benevolent, there are a lot of false positive. It is not difficult to find faces in image based on this technique and it is required to use verification process to find false results. The most important thing in this process is to set rules because of lot of variations of faces and poses.
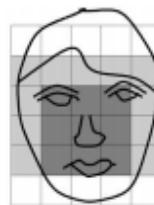
Fig. 2.   Typical face in knowledge-based methods [7]

B. Feature Invariant Approaches

Feature invariant approaches are looking for special morphological parts on face which do not change their position while movements, angles of view or lighting conditions. These methods are used mainly for locating faces in image. Feature invariant approaches are described in [7] and they are easier to implementation.

C. Template Matching Methods

Methods based on comparing templates – template matching methods need own database in which are described faces and parts of faces. Method is based on correlation between new frame and templates from local database. There is a need to update database with new faces to gain better results

and databases require a lot of storage. These methods are easier to implement and they are used mainly for face location but authors in [7] describe these methods also for face detection in image.

D. Appearance-based Methods

Template based methods have own database with faces, on the other side appearance-based methods gain and build folder with faces by learning detected faces from image. There is a training set of faces and these methods learn based on this training set. Appearance-base methods are used mainly for face detection in image. Author described these methods for face detection in [7].

E. Human Detection with History of Oriented Gradients

Method History of Oriented Gradients (HOG) is used by authors in [9][10] for human detection in image. This method is not recommended to use in real-time because of high need of system resources. There are many approaches that describe HOG in combination with other method to detect human in real-time. Author in [10] describes combination of HOG witch optical flow method. Authors in [9] propose using HOG with Kalman filter to use it in real-time.

IV. PROPOSED METHOD FOR MOTION DETECTION AND HUMAN RECOGNITION

This section of paper describes method used for software motion detection and human recognition in image sequence. Motion detection is based on analyzing each of pixels from reference image and comparing it with new image. In this paper authors use microcontroller Intel Galileo like a hardware solution.

A. Hardware Part of System

Hardware implementation is based on a development board. Authors proposed to use development board from Intel named Intel Galileo Gen 1. The device communicates with camera via IP protocol. IP camera is powered with POE 802.3af which makes it more able to move. In this implementation is used IP camera Vivotek FD7131 with resolution 640x480.

Development board Intel Galileo supports operating system Linux. Operating system is located on MicroSD card which is inserted in slot in development board. MicroSD is formatted on FAT or FAT32 and with maximum capacity of 32 GB.
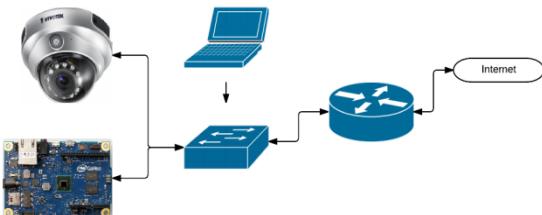
Fig. 3.   Hardware part of system for motion detection and human recognition

Fig. 3 depicts the hardware implementation of the proposed system. A computer device is used to control software and to start the program. This solution is designed to be accessible from the Internet.

B. Overall Software Implementation of Proposed System

The implementation part is based on analysis of methods for motion detection and human recognition in picture. Authors based on analysis carry out the implementation, which is composed of two parts: software motion detection and software human recognition. The main program has to be compiled directly on the device Intel Galileo and the program is written in programming language C. The program does not use any other libraries, only standard libraries from C. Software implementation is compiled on device using GNU compiler. The software part is divided to smaller following parts:

1) Installation of operating system on development board Intel Galileo using MicroSD card.

2) Configuration of IP camera and test connection between IP camera and development board.

3) Daemonize program to run in system like a process.

4) Software motion detection based on comparing two following frames.

5) Software human recognition based on analyzing frames.

6) Create web interface to show results from program and gallery with pictures with positive detection.

7) Automation of solution.

C. Implementation of Main Program

The main program has multiple parts and together they create complete solution. The main part is program to motion detection and human recognition implemented in C and compiled on development board. The main program has to serve to different parts which are:

1) Download first frame from camera which become reference image.

2) Program has cycle in which are downloaded images from camera. Program has to have access to two images in one moment. All images are saved on development board.

3) Program compare new image with reference image and all pixels are being compared.

4) If there is detected motion then system tries to recognize persons in image. If there is a person in image then image is saved and shown in gallery with positives detections.

5) Program is running as a daemon in operating system and results from motion detection and human recognition are logged in text file.

The program is running in cycle. There are two cycles. The first one is for downloading actual image from camera. The second one is used for motion detection and human recognition if needed. The main program has two parts: motion detection and human recognition.
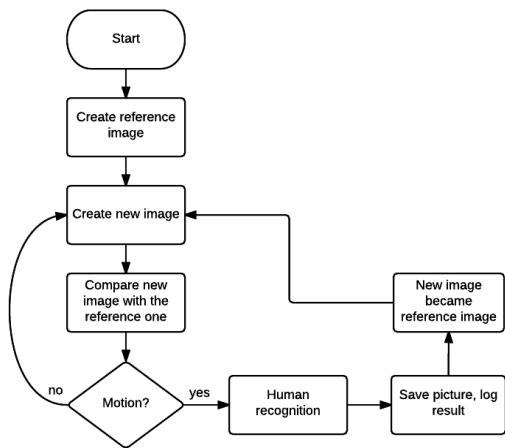
Fig. 4. Lifecycle of proposed program

Fig. 5. Modified output with marked persons

D. *Proposed Function for Motion Detection in the Two Following Video Frames*

One of two major functions of the main program is motion detection. Reference image is created after program starts and it is converted from JPEG in to BMP format in which program can works witch pixels color scales. New image from camera is downloaded in cycle. Motion detection is implemented like comparison of color scale from each pixel in following image frames. Pixel has changes if value of one of color part – red, blue or green has been changed. Value of sensitivity can be set on the start of the program. Right settings for sensitivity are very important for true motion detection in the picture. If value for sensitivity is too low, there are a lot of fake pixels detected like in a motion. On the other side, if the value is too high, pixels for detection must be changed more. One pixel has been changed if every color part has been changed in comparison with pixel from reference image in the same location. Motion is detected if there is a number of changed pixels in interval for motion detection. And based on previous function, the next function tries if there is a number of changed pixels which indicates motion detection in two following frames.

E. *Proposed Function for Human Recognition in Image*

The second function in the main program is for human recognition in picture. Human is detecting in image only if the result of motion detection is positive, on the other side, program continues with motion detection on the next image. Human recognition works on principles that the program has location of changed pictures and their count. Changed pixels must be next to themselves. The human silhouette is described in invariant parameters and program tests if the square with pixels is in shape of person. Based on testing, program knows how many pixels on image create one silhouette. Program tries to eliminate object which are not persons with different restrictions for pixels location. Silhouette is described like a square m x n. The size of square was determined by testing in different locations and in different poses. Results of this method are logged into text file with timestamp and number of counted persons. The modified output from program is shown in the Fig. 5 with marked persons who were identified by method to human recognition.

V. RESULTS AND CONCLUSION

The aim of this paper was the implementation of the system for motion detection and human recognition in video frames using development board. The system proposed by authors of this paper satisfies requirements. Development board Intel Galileo and video source from IP camera are used as a basis for the hardware implementation. Operating system Linux on the Intel Galileo development board is a good solution. However, there are not enough system resources to implement better methods for motion detection and human recognition. Authors in this implementation show the way of realization system for motion detection and human recognition on the development board. Implemented solution was tested in two different scenes to gain better results. In each scene was program tested with three different values for sensitivity to change color value of a pixel. The results show that implemented method for human recognition works. The results from two different scenes summarize the following tables:

TABLE I. HUMAN RECOGNITION TEST RESULTS: SCENE 1

Scene 1, total images: 1200, detections: 186	Low sensitivity	Medium sensitivity	High sensitivity
True positive	57 / 79%	67 / 85%	26 / 72%
False positive	15 / 21%	11 / 15%	10 / 18%

TABLE II. HUMAN RECOGNITION TEST RESULTS: SCENE 2

Scene 2, total images: 850, detections: 141	Low sensitivity	Medium sensitivity	High sensitivity
True positive	27 / 60%	46 / 82%	36 / 90%
False positive	18 / 40%	10 / 18%	4 / 10%

Two types of scenes were considered, both indoors, the first scene was a computer networks laboratory. Camera in this case was attached to the ceiling of the room. Sun light had a great impact on the number of false positives. The second room was storeroom, same as for the first scene; camera was attached to the ceiling. Number of true positives was in this case better due to better lightning conditions and lesser complexity of the room. For both cases, presence of artificial light enhanced the overall results.

In the future, we plan to eliminate just stated issue with nature light and enable utilization of system in real conditions. Implementation of a system for tracking of people in the laboratories of Technical university of Kosice is also considered, the solution itself has already been implemented as a part of the surveillance system at the university's dormitory.

REFERENCES

[1] P. Labaš, "Podklady na prijímacie skúšky z chémie", Bratislava: ELÁN, 2013, 343 p.

[2] V. Bada, "Základy klinickej elektrokardiografie", Bratislava: UK, 2010, 124 p.

[3] J.R. Hampton, "EKG stručně, jasně, přehledně", Praha 7: Grada Publishing, a.s., 2013, 192 p.

[4] M. Pytliak, "Základy kardiografie pre štúdium ošetrovateľstva a ostatné zdravotnícke študijné programy", Košice: Univerzita Pavla Jozefa Šafárika v Košiciach, 2009, 134 p.

[5] Arduino Uno [online] available at: http://arduino.cc/en/Main/arduinoBoardUno

[6] Co je to Arduino [online] available at: http://www.czechduino.cz/?co-je-to-arduino,29

[7] Vývojové prostredie a programovanie Arduina [online] available at: http://uart.cz/90/ide-a-programovani-arduina/

System for EKG Monitoring
Solution based on Arduino microcontroller

Jakub Ševčík
Dept. of Computers and Informatics
FEI TU of Kosice
Kosice, Slovak Republic

Peter Feciľak
Dept. of Computers and Informatics
FEI TU of Kosice
Kosice, Slovak Republic

Ondrej Kainz
Dept. of Computers and Informatics
FEI TU of Kosice
Kosice, Slovak Republic

František Jakab
Dept. of Computers and Informatics
FEI TU of Kosice
Kosice, Slovak Republic

Abstract—In this paper the system for the electrocardiogram (EKG) monitoring based on the of Arduino microcontroller is presented. Detailed description of the electrocardiogram itself serves as a ground for building the proposed hardware and software solution. The software implementation is in a form of both, Mat-lab environment, and own application. Final output enables retrieval of the actual data in real time and further and provide the rudimentary diagnosis. Utilization of such device is for self-home diagnosis of arrhythmia.

Keywords—Arduino; arrhythmia; C sharp; cardiovascular diseases; diagnosis; electrocardiogram; heart; Matlab

I. INTRODUCTION

Electrocardiogram machine got its popularity in the first half of the twentieth century. Examination at a cardiologist is considered these days to be nothing out of the ordinary. Despite the fact that EKG is only hundred years old, this technique is still the most reliable at determining an acute myocardial infarction (AMI). No other examination for diagnosis of such frequent and difficult problem as arrhythmia is being preferred. To make EKG machine work correctly, its proper construction and further configuration are necessary. Such device is used by people of different ages, for this reason, comfort, quick and exact usage should be provided. It is vital for the electrocardiogram to determine possible heart diseases in the shortest time possible.

The goal of this project is a construction of a machine analogous to the EKG machine and deployment of a software solution while still being able to achieve sufficient results. The brief introduction of EKG and hardware is introduced in the next sections with the subsequent rudimental implementation of both hardware and software.

II. ELECTROCARDIOGRAM IN DETAIL

People have many things in common, and the electrocardiogram is one of those, providing no physiologic or pathologic factor is present. Labaš [1] describes it is a visual record representing the changes of electric potentials in the operation of cardiac muscle. The heart is a muscle in the body with special morphologic and functional role. Bada [2] refers to the myocardium as a syncytium of muscle cells is acting as a singular muscle fiber. During irritation – depolarization, which is gradually spread from atria to ventricles the potential differences originate, so-called action flows that create the electric field of the heart being spread by the surrounding structures of lungs and muscles. Due to the sensible registration machine, these flows are recordable also from body skin. Hampton presents in his book [3] dependency of the clinical diagnosis in particular on anamnesis and a lesser extent on a physical examination of the patient. EKG, as a tool, may support a diagnosis and in some cases is crucial for a concrete treatment of the patient. However, it is essential to perceive EKG as a tool and not as a goal itself. It helps with diagnosing the pain in the chest and also the proper utilization of thrombolysis is dependent on EKG. Further, it helps with cure of a heart attack or could contribute to a diagnosis of cardiac dyspnea. As a basis for the interpretation of EKG serves a recognition of the patterns based on several rules.

According to Pytliak [4] the electrical activity of the heart is visible by changes of electrical intensity also on the surface of the body. By sufficiently sensible galvanometer the changes on the surface of the body could be measured and registered, it is a principle of the creation of the EKG record. Summation of electric displays of all the cells in the given time interval results in a changes in the intensity.

III. PHYSIOLOGICAL CURVE OF EKG

Following Bada [2], the EKG curve is made by a group of positive and negative amplitudes so-called Wavelets. These are marked as given by international convention with letters [P,Q,R,S,T,U] just as were originally named by Einthoven. Horizontal passages of the curve are called intervals. Places between intervals are called segments. Physiologically, these passages of EKG are on the level of an isoelectric line. If the horizontal passages are above the level of the isoelectric line, it is the elevation, if the horizontal passages are under the level of the isoelectric line, it is the depression. Wavelets located above the level of the isoelectric line are called positive, and those under the level of the isoelectric line are called negative. Wavelets of which one part is positive and the second one negative are diphasic. Next, the relevant waves, intervals, and segments are described.

A. P wave

This wave is a sign of depolarization (contraction) of atrial muscle and also is the main criterion of the sinusoidal rhythm – when the initial impulse originated in the sinoatrial node and from there was carried to the atrial muscles.

B. Interval P-Q

From the beginning of the P wavelet to the beginning of the Q wavelet (if the wavelet Q is missing, then to the beginning of the wavelet R). This interval represents the time it takes for depolarization to spread over the muscle of the atria and the ventricles to the level of Purkinje fibers, this is referred to as a conversion time.

C. Q wave

This is the first negative wave after P wavelet or the first negative wave before the R wave. It is start of the ventricular complex and reflects the course of the depolarization of the interventricular barrier, which is of the whole ventricular muscle depolarized as the first one. Physiological Q wave tend to be just schematic, its absence is not pathological.

D. Q,R,S waves

Together they form the so-called initial ventricular complex of the same name, which reflects the depolarization of the ventricular muscle. It is bordered by the beginning of Q wave and ends with S wave.

E. S-T segment

This segment is the section from the end of the S-wave, where ends the ventricular QRS complex (J point) and the beginning of the T wave. Under physiological conditions, the S-T segment is on the level of the isoelectric line and reflects the early phase of repolarization of the ventricular muscle.

F. T wave

T wave has the same course as the ventricular complex, it is positive where the ventricular complex is positive. The T wave is a reflection of repolarization of the atrial muscles, thus it is always shown in the EKG. If the T wave is not present in the EKG, we say that it is on the level of the isoelectric line.

G. U wave

This wave is a non-constant part of the ECG curve, it tends to act as a small positive deflection behind wave. It is a reflection of so-called delayed repolarization of ventricular muscle. Lacking of U waves is never pathological. This wave is present in the EKG record from athletes.

H. Q-T interval

Interval, also known as electrical systole of heart, represents the time from the beginning of the ventricular QRS complex, i.e. from the beginning of the Q wave (in its absence from the beginning of the R wave) till the end of the T wave. It is a conclusion of depolarization and repolarization of the ventricular muscle. QT interval particularly depends on the heart rate.

IV. ARDUINO MICROCONTROLLER

Arduino is an open electronic platform [6], the principal reason of its success is user friendly hardware and software.

Arduino is able to perceive the environment by utilizing various sensors and shields that may be connected to it. Arduino is a massive development kit based on the microprocessor ATMEGA328 and contains 13 digital input-output pins, 6 of them with support of pulse-width modulation (PWM) and 6 analog inputs [6]. Among all the free computer platforms for electronic projects such as Galileo or Raspberry was for this project chosen Arduino due to specific aspects, i.e. in conjunction with ECG it overruns other projects. Other aspects are: clearly and easily usable API with a simple programming language, then so-called Arduino shields that actually represent enhancements of the Arduino board [7]. Note that some of these shields are directly created for the purpose of human sensing signals. This very idea is the essential for our purpose, since it is possible to make own shield or to acquire already existing one. In our case, the shield provided by the Olimex is being utilized, bearing in mind the need to extract the highest possible signal quality. EKG shield can be connected in various ways, among the most basic are 12 - lead ECG.

V. HARDWARE IMPLEMENTATION

Based on the reviews of the available literature dealing with the EKG, and after comparative analysis of the options available to create an EKG device similar to a medical one, it was decided to utilize: Arduino UNO, shield Olimex EKG, electrodes designed for ECG shield. For signal processing is utilized Matlab environment and own software solution was also created.

As already stated, the project consists of two principal parts, i.e. hardware and software. In the hardware part, Arduino UNO with ECG Shield was combined. These two devices fit together very well. After their engagement in individual pins, Arduino was upgraded by the opportunity to capture the signals of the heart. Arduino was constantly connected to computer device and by this the need to use external battery was omitted, note that the energy was supplied through USB. It was proposed that that the EKG data is to be plotted directly on the screen using Matlab environment and our application. This condition removed necessity to use SD card for data recording, also use of mini displays or oscilloscope displays.

A. Electrodes

The original EKG devices used in medical practice in the art of cardiology use a combination of different electrodes. They combine electrodes connected to the legs, specifically to the ankles and wrists and electrodes that are attached directly to the chest near the heart. This project utilized electrodes from Olimex, which are also suitable for operation with Olimex shield. These electrodes are created exactly for connection in the form of Einthoven triangle. This type of connection includes three electrodes - one on the right hand, the second one on the left hand and the third one on the left leg. Three electrodes cross the notional heart. The right foot is taken as connection to the ground. Electrodes have also the option of renewable terminals. Terminals are affordable, thus a new set of terminals may be used for each tested person. The electrodes are connected directly to the ECG/EMG shield, specifically to the electrode jack.
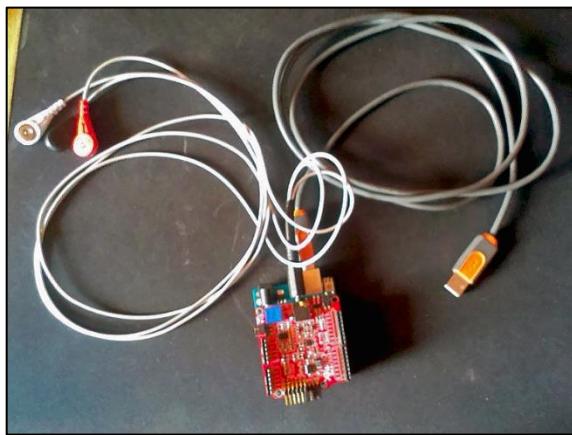
Fig. 1. Arduino, EKG shield and connected electrodes

Note that we can connect just one type of electrodes for a shield. Hardware component is depicted in the Fig. 1.

VI. SOFTWARE IMPLEMENTATION

Software part utilized Matlab environment to output the direct sinusoid, specifically Matlab Data Acquisition Toolbox was used. Another approach included development of own secondary application, where the signals from the Arduino microcontroller were filtered and analyzed, note that application was developed in in C# language.

A. Matlab environemnt

In this case was created a simulation in which was simulated the RAW Arduino output via acquisition toolbox, which directly cooperates with the Arduino boards. In the simulation, specific COM port was selected to enable receiving of data and further is was opened. The entire simulation was portrayed in the cycle and a result was a graph. Graph itself was rather of chaotic nature, since we received input data from the RAW input along with noise.

B. Secondary application

The application can render down real-time ECG signal that can be filtered, also performs the calculation of the heart rate and enables detection of arrhythmia.

In the course of project, two programming languages for application development were considered, i.e. Java or C sharp. Both, Java and C Sharp, utilize RXTX libraries that can cooperate directly with Arduino boards. It was found that C sharp provides more advanced pre-build parts and principles that fit out needs. C sharp and Java in combination with Arduino facilitate us to connect Arduino to the USB port of the computer device and further its COM port can be found in the application. Once the COM port exists and is defined correctly, the application can send/receive messages from Arduino microcontroller. Communication takes place via the so-called serial interface. Main reason for utilization of C sharp was due to possibility of utilizing the advanced mathematical filters. These filters were in C sharp very well analyzed, and for this reason assisted in the implementation of the application in a significant way. The package OLIMEXINO-328 was used as well and helped in better synchronization with the shield.
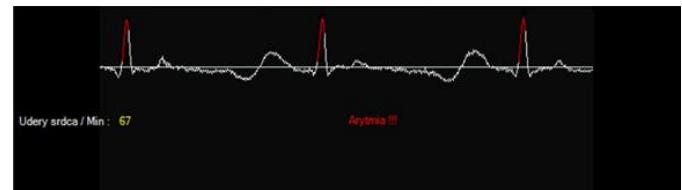
Fig. 2. Screen of application: Successful diagnosis

Screenshot of the secondary application is depicted in the Fig. 2.

Two types of filters were utilized:

1) Butterworth filter

Butterworth filter is a filter type for signal processing designed to provide the biggest possible flat frequency response. This is known as the maximum flat dimension filter. Originally it was described in 1930 by British engineer and physicist Stephen Butterworth.

2) Haar wavelet

Haar wave is a sequence recounting "square" functions, which form together a wavelet family or basis. Haar analysis is similar to Fourier analysis in allowing the target function in the interval to be expressed as an orthonormal function. The sequence of Haar was designed in 1909 by Alfred Haar.

C. Structure of secondary application

Application consists of eight main classes with basic Properties, References and app.configuration already included. Two of the principal classes are the classes of filters, one is for transformation, and the next one limits the size of the curves. Furthermore, there are classes for rendering down curves in real-time diagnostics, a class where the basic settings are and as the last one there is the main class.

Haar class creates a Haar wavelet filter. In this class there are three methods. First method is the one, which triggers a recursive method for calculating the Haar transform. The result of Haar transformation is a single integral number and a vector of coefficients. These coefficients are calculated from the highest to the lowest frequency however the Haar functions other way around, and therefore, we have a method which makes the inversion. The third method triggers the first two mentioned methods. Butter Worth is a class representing Butterworth filter. This class contains just one method, which takes information from the Fourier transformation of the class Fourier.cs. Consequently, a calculation to the original is in the progress. This method contains the conditions for the upper and lower limit of the filter. Fourier class contains an algorithm for calculation of fast Fourier transformation. Strop is class that sets scaling of the curve. The Class contains two methods. One method involves rendering down size of the curves. It also contains a condition for turning on and off scaling option. The second method runs in a cycle, and calls for the first one. Real Time is a class that contains a rendering of a curve in the real time. This class works with the package OLIMEXINO-328th. The main cycle can be found here, it receives information from the Arduino. Furthermore, there are cycles for applying Haar and Butterworth filters. In this class there are also saved settings for our filters along with scaling of the

curve. There are also defined portrayals e.g. colors of lines and background, list of the heartbeat and the arrhythmia. Class called Diag deals directly with heartbeats and arrhythmia detection. Every single heartbeat can be detected and average heart rate calculated by the number of strokes per chosen time, which we calculate by the time between heartbeats and then convert it to a period of one minute. Arrhythmia is detected according to the time between heartbeats. If the time period is different between certain strokes, then it is evaluated as arrhythmia. Another class used was for communication with a serial port. This class concerns a method, which opens the COM port, which is from the beginning defined on COM.

D. Conclusion

The principal goal of this project was the construction and configuration the EKG-based device on Arduino microcontroller with an emphasis on its ease in controlling and applicability in routine practice, whether to professionals or the laymen. People are usually pretty familiar with EKG machine, which is used by cardiologists worldwide to determine different heart defects. Cardiovascular diseases take the top places in the list of the civilization diseases, one of the most common being the myocardial infarction (AMI). Such serious illnesses can be avoided by early diagnosis e.g. thanks to the devices such as EKG machine based on the Arduino.

The aforementioned sections introduced the advantage of this device being a quick diagnosing of cardiac arrhythmia. Generally, this examination is painless, and the patient has sufficient comfort and convenience. The greatest benefit would be for patients who need an immediate record of their health from the home. This benefit is the very consideration taken into account when developing such a device.

The disadvantages and related possible future improvements are the limited ability of the diagnosis since the exact type of arrhythmia cannot be determined. Next being the lack of storage of our measurement to a file or even lack of uploading it somewhere on the internet. However probably the biggest disadvantage of the current device is a large inaccuracy compared to the original EKG medical devices used in hospitals. These are the main concerns to be the principal focus in the future research.

REFERENCES

[1] P. Labaš, "Podklady na prijímacie skúšky z chémie", Bratislava: ELÁN, 2013, 343 p.

[2] V. Bada, "Základy klinickej elektrokardiografie", Bratislava: UK, 2010, 124 p.

[3] J.R. Hampton, "EKG stručně, jasně, přehledně", Praha 7: Grada Publishing, a.s., 2013, 192 p.

[4] M. Pytliak, "Základy kardiografie pre štúdium ošetrovateľstva a ostatné zdravotnícke študijné programy", Košice: Univerzita Pavla Jozefa Šafárika v Košiciach, 2009, 134 p.

[5] Arduino Uno [online] available at: http://arduino.cc/en/Main/arduinoBoardUno

[6] Co je to Arduino [online] available at: http://www.czechduino.cz/?co-je-to-arduino,29

[7] Vývojové prostredie a programovanie Arduina [online] available at: http://uart.cz/90/ide-a-programovani-arduina/

Automatic Recognition of Human Parasite Cysts on Microscopic Stools Images using Principal Component Analysis and Probabilistic Neural Network

Beaudelaire Saha Tchinda
Laboratoire d'Automatique et
d'Informatique Appliquée (LAIA),
IUT-FV de Bandjoun, Université de
Dschang-Cameroun, B.P. 134
Bandjoun

Daniel Tchiotsop
Laboratoire d'Automatique et
d'Informatique Appliquée (LAIA),
IUT-FV de Bandjoun, Université de
Dschang-Cameroun, B.P. 134
Bandjoun

René Tchinda
Laboratoire d'Ingénierie des
Systèmes Industriels et de
l'Environnement (LISIE), IUT-FV
de Bandjoun, Université de Dschang-
Cameroun, B.P. 134 Bandjoun

Didier WOLF
CRAN UMR CNRS 7039, ENSEM Université de Lorraine,
Nancy, France.

Michel NOUBOM
Département des sciences Biomédicales, Faculté des
sciences, Université de Dschang

Abstract—**Parasites live in a host and get its food from or at the expensive of that host. Cysts represent a form of resistance and spread of parasites. The manual diagnosis of microscopic stools images is time-consuming and depends on the human expert. In this paper, we propose an automatic recognition system that can be used to identify various intestinal parasite cysts from their microscopic digital images. We employ image pixel feature to train the probabilistic neural networks (PNN). Probabilistic neural networks are suitable for classification problems. The main novelty is the use of features vectors extracted directly from the image pixel. For this goal, microscopic images are previously segmented to separate the parasite image from the background. The extracted parasite is then resized to 12x12 image features vector. For dimensionality reduction, the principal component analysis basis projection has been used. 12x12 extracted features were orthogonalized into two principal components variables that consist the input vector of the PNN. The PNN is trained using 540 microscopic images of the parasite. The proposed approach was tested successfully on 540 samples of protozoan cysts obtained from 9 kinds of intestinal parasites.**

Keywords—Human Parasite Cysts; Microscopic image; Segmentation; Parasite extraction; feature extraction; Principal component analysis; probabilistic neural Network; Parasite Recognition

I. INTRODUCTION

The intestinal parasite is a form of human parasite. It is one cause of medical consultations in tropical countries, especially in underdeveloped countries. It was estimated about to 4 billion the number of people infected worldwide [1]. This pathology causes death or physical and mental disorders in children and immune-deficient individuals [1]. The diagnosis of parasitical diseases is performed in the laboratory by the visualization of stools samples through the optical microscopy. Intestinal

parasites are classified taxonomically into protozoa and helminths. The protozoa can be seen in stools either on the vegetative form or as the resistant cyst. Helminths are found in the stool in the statement of eggs or larvae. The identification of a parasite is done by the comparison of the morphology observed with the known shapes. This practice is very tedious and is not without consequences for the eyes of laboratory technicians. Also, it is time-consuming and is subject to many diagnosis errors. The identification of amoebic cysts remains the most difficult. Indeed, the cysts are smaller than the helminth eggs, and their distinguishing criteria are more complex. Unlike helminths for which the size is a determinant parameter distinction, many amoeba cysts have almost the same dimensions, and we must use other types of parameters such as the number of the nucleus, for example, to identify them.

During the last decades, several studies employed microscopic image analysis to automatically diagnose the human parasites [2; 3; 4]. Since many parasitic organisms present developmental stages that have a well-defined and reasonably homogeneous morphology, they are amenable to pattern recognition techniques. Each study can be distinguishing from other by the species of parasite concern in the classification, the classification tools and the type of feature using by the classifier. Yang et al. [2] addressed the identification of human helminth eggs by artificial neural network (ANN). Avci et al. [3] and Dogantekin et al. [4] addressed the recognition of human helminth eggs using support vector machines (SVMs) and a fuzzy inference system based on adaptive network, respectively. While these methods are limited to helminths, Castanon et al. [5] used Bayesian classification for the identification of seven species of Eimeria (a protozoan of the domestic fowl); Ginoris et al. [6; 7] used ANN to recognize protozoa and metazoa that are typically

found in sludge; and Widmer et al. [8] addressed the identification of Cryptosporidium oocysts and Giardia cysts in water using ANN and immunofluorescence microscopy. These works, however, do not address the identification of human intestinal protozoa in feces, and the segmentation of the parasites is manual. Recently, Suzuki et al. [9] proposed a first solution for automatic identification of the 15 most common species of protozoa and helminths in Brazil.

In this paper, we propose an automated method of human parasite diagnosis via image analysis and an artificial neural network system. Our approach relies on three main steps after image acquisition: edge detection, image segmentation and object recognition. In [10] and [11], we proposed a solution for the two first steps. The present work focuses on the parasite recognition using the results of the precedent works. The main difference of our method from the previously parasite recognition method is the type of feature descriptor used in this work. Our feature descriptor uses the image pixel directly and not need to process other parameters from this image. Our classification tool combines principal component analysis (PCA) for dimensionality reduction and Probabilistic neural network. Our method was applied successfully on nine amoebic cysts types.

The rest of the paper is organized as follow. In section 2, we describe the principles of the methodology. The algorithms of parasite recognition are described in section 3. Experimental results are presented and discussed in section 4. Finally, section 5 presents the conclusions of the work.

II. Methods

A. Edge detection, image segmentation and parasite extraction

Parasite extraction is a crucial step preceding the recognition. An image may contain multiple parasites and we need to identify them individually. Object extraction consists to separate the image region of interest (ROI) from it background. This is done after the segmentation process. The common methods of segmentation can be divided into two categories: the method based on the region and method based on contours. The region oriented segmentation is based on the intrinsic properties of objects to be extracted. This method is highly dependent on the characteristics of the image and shape to extract. The method using contours consists to seek the boundaries of the region to be extracted by exploiting the discontinuity of intensity levels. The usual techniques of edge detection are based on either the gradient or the Laplacian of the image intensity function. We distinguish the following detectors: Sobel, Robert, Prewitt, and Canny. It is shown in [10] that the edge detection based on multi-scale wavelet is better than the other classic detectors when applying on the microscopy image of intestinal parasite. The other advantage for applying the wavelet transform to the detection of edges in an image is the possibility of choosing the size of the details that will be detected [10].The Hough transform has the ability to extract the parametric forms in an image. The Hough Transform has been applied to a wide variety of problems in machine vision, including: line detection, circle detection, detection of general outlines, the detection of surfaces and the estimation of 2 and 3-D motion. The Hough transform (HT)

has been used in [12] to segment ultrasound images of longitudinal and transverse sections of the carotid artery. Certain intestinal parasites are circular in its shape. The circular Hough transform can be easily used to locate and extract them. However the location of other random forms remains partial. Another segmentation method uses the active contours model. The active contour method is very effective for the detection of boundaries. An example of the active contours model implementation is presented in [13]. The strong dependence on initial contour has long been considered as its main drawback. An initial contour close to the target contour promotes greater convergence. It is possible to combine the technique of Hough transform to the active contour technique. The Hough transform allows to this new method to automatically locate the region of interest of the parasite. This first result will be the initial contour for active contours model. This approach had been used successfully in [11] to extract intestinal parasites on the microscopy images.

The first step is the edge detection obtained from the multi-scale wavelet transform. The second step process the circular Hough transform from the edge. In this step, each edge element votes for all the circles that it could lie on and the circle corresponding to the maximum vote is retained. This circle locates the region of interest around of which the parasite is situated. In the third step, the active contour based on gradient vector flow model is computed. The active contour uses the circle obtained from the Hough transform as its initial contour. This initial contour is deformed and attracted towards the target contour by various forces that control the shape and location of the snake within the image. The last step uses the final contour to get the mask corresponding to the interior of the area delimited by the contour. The parasite extracted corresponds to a logic operation of the mask with the original image. Besides the microscopic image, our scheme also use as input the length of the radius to find the parasite, the number of convolutions (analyzing scale) to find the edge map by the multi-scale wavelet transform and the threshold of the edge detection. The detailed version of the parasite extraction algorithm can be seen in [11].

B. Feature extraction and dimensionality reduction

Feature extraction aims to represent candidate objects with a simple and representative manner to discriminate an object from other. There is several type of feature descriptor [14]. The main difference of our method in relation to the previously parasite recognition method is the type of feature descriptor used in this work. Our feature descriptor uses the image pixel directly and not need to process other parameters from this image. The dimension of such vectors is very large. There is the need to map those vectors to the lower dimensional space; thereby reducing the computational complexity for further classification. The feature dimension reduction consists of mapping the input vectors of observations $I \in \mathbb{R}^m$ onto a new feature description $X \in \mathbb{R}^n$, with $n < m$. The dimensionality reduction based on the projection technique is considered on this paper. The projection technique is achieved by using transformation matrix M. The Principal Component Analysis (PCA) is a representative of the unsupervised learning method which yields the linear projection [15; 16].

Let consider an input vector $I \in \mathbb{R}^m$ which need to be mapping onto a new feature description $X \in \mathbb{R}^n$. The projection is given by the matrix $M[m \times n]$ and the bias vector $k[n \times 1]$.

Let $T_I = \{I_1, ..., I_l\}$ be a set of training vector from the m-dimensional input space $\mathbb{R}^m$.

$$T_I = \begin{cases} I_1 = [I_{11}, I_{12}, ... I_{1m}]^T \\ . \\ . \\ . \\ I_l = [I_{l1}, I_{l2}, ... I_{lm}]^T \end{cases} \qquad (1)$$

The set of vectors $T_X = \{X_1, ..., X_l\}$ is a lower dimensional representation of the input training vectors T_I in the n-dimensional space $\mathbb{R}^n$.

$$T_X = \begin{cases} X_1 = [X_{11}, X_{12}, ... X_{1n}]^T \\ . \\ . \\ . \\ X_l = [X_{l1}, X_{l2}, ... X_{ln}]^T \end{cases} \qquad (2)$$

The vectors of T_X are obtained by the linear orthonormal projection

$$X = M^T I + k, \qquad (3)$$

where the matrix M and the vector k are parameters of the projection. The reconstruction vector $T_{\tilde{I}} = \{\tilde{I}_1, ..., \tilde{I}_l\}$ are computed by the linear back projection

$$\tilde{I} = M(X - k), \qquad (4)$$

obtained by inverting (3). The mean square reconstruction error

$$e_{MS}(M, k) = \frac{1}{l} \sum_{i=1}^{l} \|I_i - \tilde{I}_i\|^2, \qquad (5)$$

is a function of the parameters of the linear projections (3) and (4). The principal component analysis is the linear orthonormal projection (3) which allows for the minimal mean square reconstruction error (5) of the training data T_I. The parameters (M, k) of the linear projection are the solution of the optimization task

$$(M, k) = \underset{M', k'}{\arg\min}(e_{MS}(M', k')), \qquad (6)$$

such as $\langle M_i . M_j \rangle = \delta(i, j), \ \forall i, j \in \mathbb{N}$,

where $M_i, \ i = 1, ..., n$ are column vectors of the matrix $M = [M_1, ..., M_n]$ and $\delta(i, j)$ is the Kronecker delta function. The solution of (6) is the matrix $M = [M_1, ..., M_n]$ containing the n eigenvectors of the sample covariance matrix which have the largest eigen values. The vector k equals to $M^T \mu$, where μ is the sample mean of the training data. The PCA is treated throughout for instance in [17].

C. Object classification using the Artificial Neural Network

Artificial Neural Networks are analogous to their namesake, biological neural networks, in that both receive multiple inputs and respond with a single output. ANN classifies input vector into a specific class according to the maximum probability to be correct. These networks have diverse applications in machine vision [18]. One of their applications is in classification and decision making based on existing data [19]. For this goal, the input data is often divided into two parts for training and testing.

In an ANN, multiple neurons are interconnected to form a network and facilitate distributed computing. Each neuron partition constitutes a layer. Networks may contain an input layer, an output layer, and a hidden inner layer. Additional hidden layers may be added to increase the complexity of the network. Weights are assigned to each of the links between neurons, and they are updated as part of the learning process.

The configuration of the interconnections can be described efficiently with a directed graph. A directed graph consists of nodes and directed arcs. The topology of the graph can be categorized as either acyclic or cyclic [20; 21]. A neural network with acyclic topology consists of no feedback loops. Such an acyclic neural network is often used to approximate a nonlinear mapping between its inputs and outputs. A neural network with cyclic topology contains at least one cycle formed by directed arcs. Such a neural network is also known as a recurrent network. Due to the feedback loop, a recurrent network leads to a nonlinear dynamic system model that contains internal memory. Recurrent neural networks often exhibit complex behaviors and remain an active research topic in the field of artificial neural networks. Network topology architecture was systematically chosen in terms of variance of classification results and its complexity. The Probabilistic Neural Networks (PNN) is used in this paper to classify the type of intestinal parasite. This choice is adopted for its advantages [22]. The main advantage of PNN is that training is easy and instantaneous [23; 24; 25]. The architecture for this system is shown in Fig.1. We adopt the symbols and notations used in the book "neural network toolbox for use in Matlab" [26].
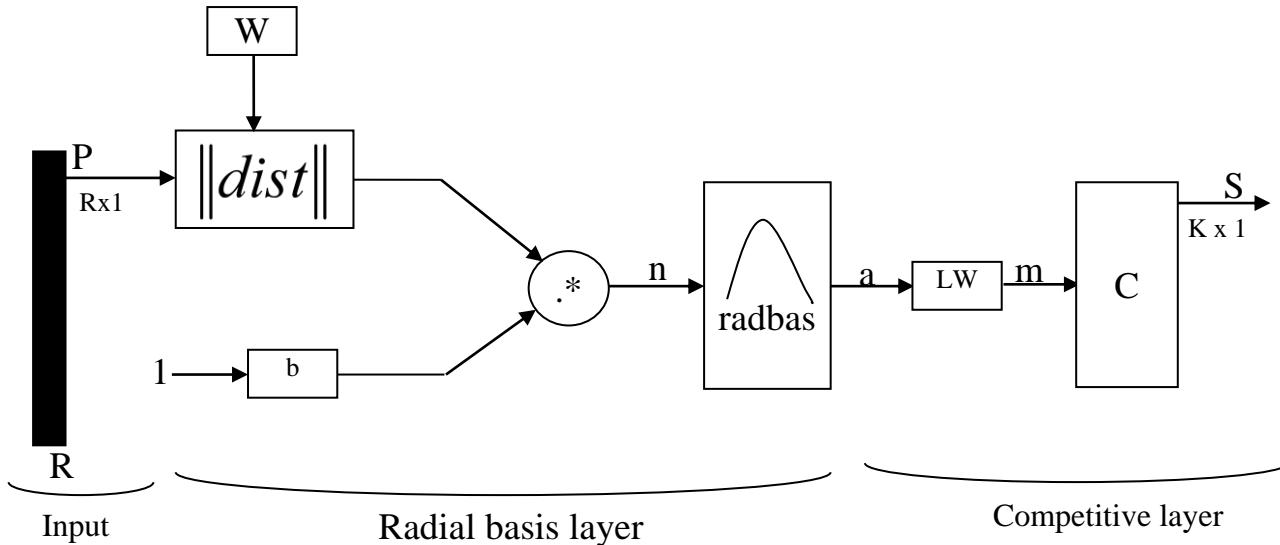
Fig. 1.   Neural Network architecture

Our PNN has three layers: the Input layer, Radial Basis Layer and the Competitive Layer.

The input layer has two units, corresponding to the two features. The input vector, denoted as P, is presented as the black vertical bar in Fig. 1. Its number of element R corresponds to the number of neurons in the Radial Basis Layer.

In Radial Basis Layer, the vector distances between input vector P and the weight vector W is calculated. This operation is represented in the Fig. 1 by the $\|dist\|$ box and its output gives $\|W - P\|$. The bias vector b and the output $\|W - P\|$ are combined by an element-by-element multiplication, represented as ".*" in Fig.1. The result is denoted as $n = \|W - P\|.*b$. The transfer function in the radial basis network is define as

$$radbas(n) = \exp(-n^2) \qquad (7)$$

Each element of n is substituted into (7) and produces corresponding element of a, the output vector of Radial Basis Layer. We can represent the i-th element of a as

$$a_i = radbas(\|W_i - p\|.*b_i) \qquad (8)$$

where Wi is the vector made of the i-th row of W and b_i is the i-th element of bias vector b. An input vector close to a training vector is represented by a number close to 1 in the output vector a. If an input is close to several training vectors of a single class, it is represented by several elements of a that are close to 1.

The competition layer classifies each input in each of the K class of protozoan cysts use during the training phase. There is no bias in the competitive layer. In competitive layer, the vector a is firstly multiplied with layer weight matrix LW, producing an output vector m. The competitive function, denoted as C in Fig. 1, produces a 1 corresponding to the

largest element of m, and O's elsewhere. The output vector of competitive function is denoted as S. The index of K in the output is the number of parasite that our system can classify. It can be use as the index to look for scientific name of the parasite. The dimension of output vector is K=9 in this paper.

III.   SYSTEM ARCHITECTURE
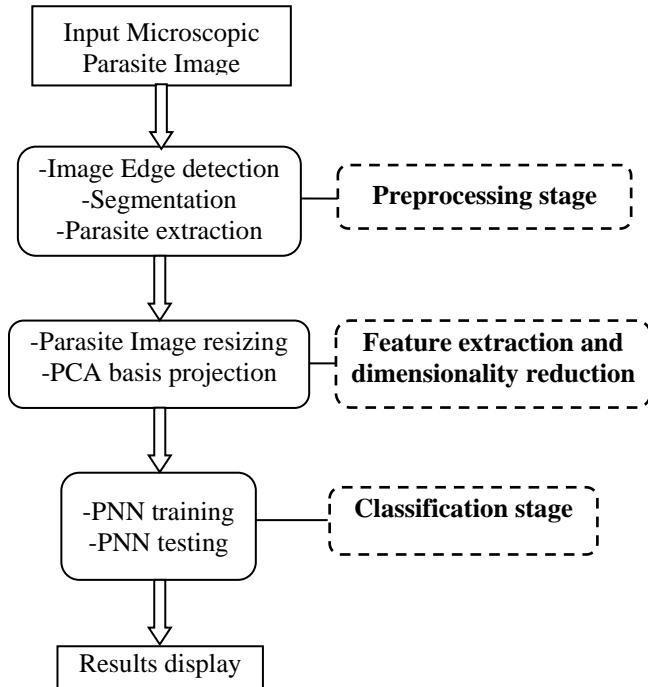
Fig. 2.   The overall processing stages of proposed scheme for intestinal human parasite diagnosis

The main goal of this work is to recognize the types of intestinal parasites in the microscopic image of stools. To achieve this purpose, a block diagram is designed based on this type of dataset. Specially, we focus on the classification and recognition of nine types of protozoan cysts. The block diagram of the proposed scheme is illustrated in the Fig. 2. As

indicated in the figure, this method has the following main steps:

Step1: image edge detection, segmentation and parasite extraction

Step 2: feature extraction and dimensionality reduction

Step 3: classification and recognition

These steps are explained in the following sections.

A. *Step1: image edge detection, segmentation and parasite extraction*
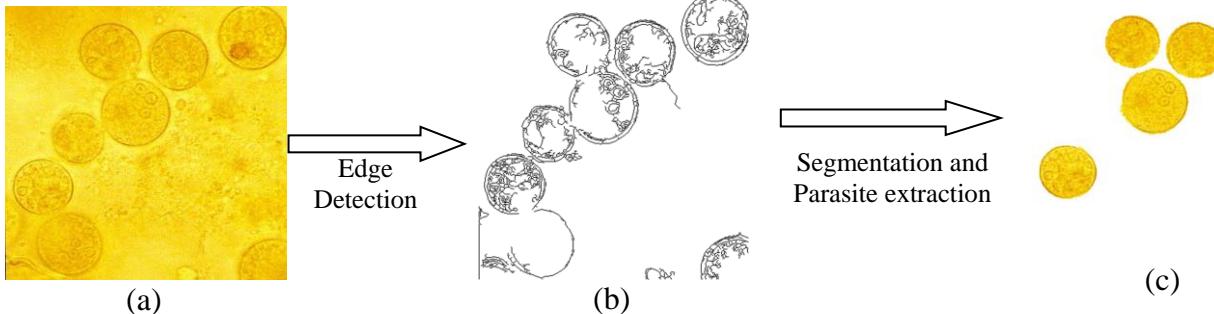
Fig. 3.   Representative illustration of a microscopic image preprocessing. (a) Microscopic image of stools, (b) image of edge detected, (c) image of the extracted parasites

Since in an image, we can have several objects which cannot be necessary interest us. Also, image can contain different parasites. We need to extract individually a parasite before the recognition. The parasite extraction is doing via the image segmentation. The segmentation use the contour edge map of the image to separate the parasite from is background. A logic operation is used to suppress the parasite background. Our segmentation method is based on the active contour initialized by the Hough transform. The edge detection method is based on the multi-scale wavelet transform. The Fig. 3 presents the illustration of the edge detection, parasite segmentation and extraction on an image containing protozoan parasite cysts.

B. *Step 2: image resizing, feature extraction and dimensionality reducing*

Fig. 4.   Two dimensionality projection with two Eigen vectors corresponding to the largest two Eigen values in PCA basis

Our feature descriptor uses the image pixel and does not need to process other parameters from this image. Nevertheless, the image needs to be resized. All image dimension of the extracted parasite has been reduced to the size 12x12. The resizing uses the Bicubic interpolation method. With this method, the output pixel value is a weighted average of pixels in the nearest 4-by-4 neighborhood.

In order to reduce the complexity of the classification and recognition phase, the feature using as input need to be reduced. PCA is used to project the 12x12 features on the new feature space. The goal of PCA is to reduce the dimensionality of the data space (12x12) to smaller intrinsic dimensionality of feature space, which is needed to describe the data economically. For this purpose, the dimensionality of the new feature space is chosen according to the classification rate and the system complexity. In this paper, the first 2 principal components have been used. When using our algorithm, one can use the mapping $f : \mathbb{R}^{144} \rightarrow \mathbb{R}^2$ to obtain the values of components in the new coordinate system. The Fig. 4 shows the result obtained in the two dimensionality projection with two Eigen vectors corresponding to the largest two Eigen values in PCA basis. This transformation is applied on 20 trained images of each of the nine types of parasite. In this figure, we can distinct the nine types of parasite. Also, as shown in this figure, each type of parasite is grouped separately from other. The capability of the new features in separating of the 9 classes of parasites can be qualitatively evaluated.

C. Step 3: parasite classification and recognition

In this phase, the reduced features are applied to train and test the neural network. Totally 1080 microscopic images of protozoan cysts are used. These samples were divided in 540, with 60 of each type of 9 parasites for training, and 540 for the test.

For our neural network training, Radial Basis Layer Weights is set to the transpose of R x Q matrix of Q training vectors. Each row of W consists of 2 principal variables of one training samples. Since 540 samples are used for training. In this paper, Q = 540.

In radial basis layer, all biases are all set to $\sqrt{-\ln 0.5}/s$ resulting in radial basis functions that cross 0.5 at weighted inputs of ±s. s is called the spread constant of PNN.

Competitive Layer Weights LW is set to K x Q matrix of Q target class vectors. K is the dimension of the output vector, equal to 9 in this paper. The target class vectors are converted from class indices corresponding to input vectors. This process generates a sparse matrix of vectors, with one 1 in each column, as indicated by indices.

IV. EXPERIMENTAL RESULTS
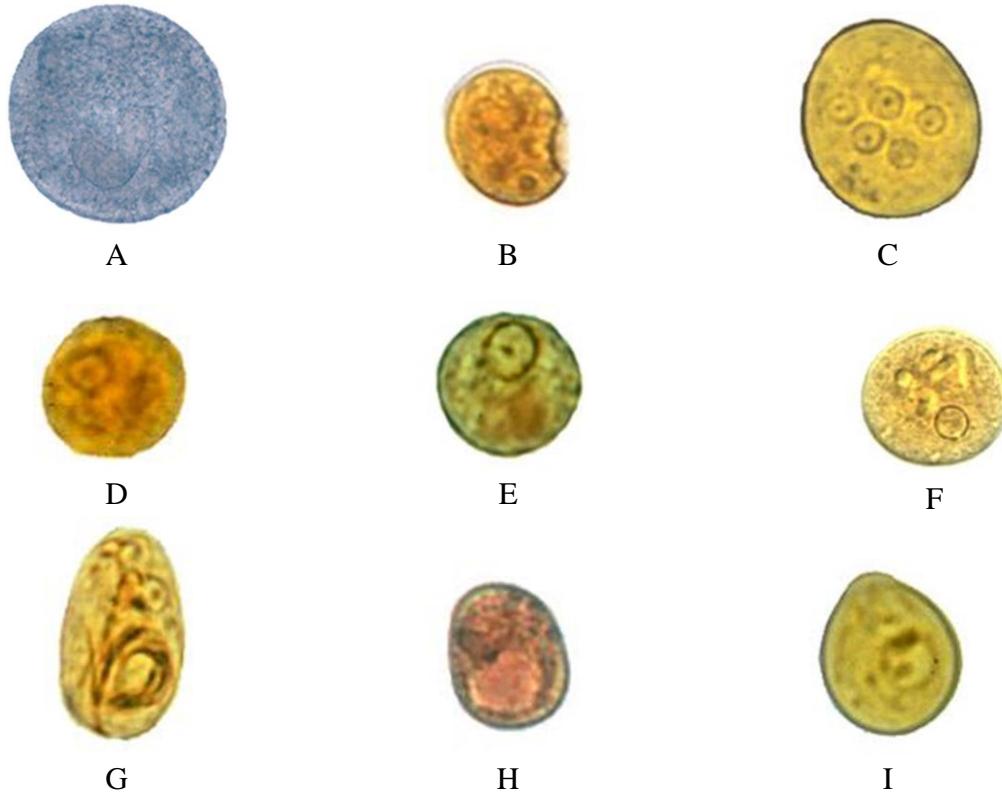
Fig. 5. Digital microscopic images of each of parasite cyst types. A: BALANTIDIUM COLI; B: ENDOLIMAX NANA; C: ENTAMOEBA COLI; D: ENTAMOEBA HARTMANNI; E: ENTAMOBA HISTOLYTICA; F: ENTAMOEBA POLECKI; G: GIARDIA LAMBLIA; H: IODAMOEBA BUTSCHLII; I: CHILOMASTIX MESNILI

In this experimental study, 9 different types of human parasite cyst are used. These types of parasite are: BALANTIDIUM COLI, ENDOLIMAX NANA, ENTAMOEBA COLI, ENTAMOEBA HARTMANNI, ENTAMOEBA HISTOLYTICA, ENTAMOEBA POLECKI, GIARDIA LAMBLIA, IODAMOEBA BUTSCHLII, and CHILOMASTIX MESNILI. Digital microscopic images of each of parasite cyst types are given in Fig.5.

All these parasite cysts are rotated in steps of 30° from 0°-150, five different scales were chosen. Also, these images were bruited with 4 types of image noise ('Gaussian', 'Poisson', 'salt & pepper', 'speckle'). In this way, 120 microscopic images were obtained for each parasite cysts types. For training the classifier, randomly chosen half of the database was used. The spread parameter was chosen to 0.4, for the best performance, after several different experiments.

The rest of the database was used in testing stage. For each kind of parasite, 60 pieces of cyst are used to test the accuracy of our algorithm. The confusion matrix of the proposed expert diagnosis system is shown in table 1. As shown in table 1, all the nine parasite cysts type images were classify with 100 % correct classification rate. This demonstrates the effectiveness of the proposed feature descriptor in the protozoan cyst recognition system based on the principal component analysis and the probabilistic neural network.

TABLE I. CONFUSION MATRIX OF THE CLASSIFICATION SCHEME

	Predicted class								
Class	A	B	C	D	E	F	G	H	I
A	60	0	0	0	0	0	0	0	0
B	0	60	0	0	0	0	0	0	0
C	0	0	60	0	0	0	0	0	0
D	0	0	0	60	0	0	0	0	0
E	0	0	0	0	60	0	0	0	0
F	0	0	0	0	0	60	0	0	0
G	0	0	0	0	0	0	60	0	0
H	0	0	0	0	0	0	0	60	0
I	0	0	0	0	0	0	0	0	60

(Actual class)

V. CONCLUSION

This paper presented an image analysis system to recognize nine kinds of human parasites. Artificial Neural Network can classify automatically the intestinal parasite via the microscopic images of stools loaded from digital cameras or scanner. The probabilistic neural network is adopted for hit has fast speed on training and simple structure. Contrary to previous work, 12x12 features vectors were obtained directly from image pixel. This features that form the input vector of PNN have been projected in a Principal Component Analysis basis for dimensionality reduction.

Results indicate that the image pixel features of microscopic image of human parasites are achievable, and it offers remarkable accuracy when using in a probabilistic neural network classifier with dimensionality reduction of the features by projection on the PCA basis. Further works will be focused on the recognition of other types of human parasites.

REFERENCES

[1] World Health Organization (2010). Working to overcome the global impact of neglected tropical diseases. First WHO report on neglected tropical diseases.

[2] Yang, Y. S., Park, D. K., Kim, H. C., Choi, M., & Chai, J. (2001). Automatic identification of human helminthes eggs on microscopic fecal specimens using digital image processing and an artificial neural network. IEEE Transactions on Biomedical Engineering, 48(6), 718–730.

[3] Avci, D. Varol, A. (2009). An expert diagnosis system for classification of human parasite eggs based on multi- class SVM. Expert Systems with Applications, 36(1), 43–48.

[4] Dogantekin, E., Yilmaz, M., Dogantekin, A., Avci, E. and Sengur, A. (2008). Arobust technique based on invariant moments—ANFIS for recognition of human parasite eggs in microscopic images. Expert Syst. Appl., 35(3), 728–738.

[5] Castanon, C. A. B., Fraga, J. S., Fernandez, S., Gruber A. and Costa L. da F. (2007). Biological shape characterization for automatic image recognition and diagnosis of protozoan parasites of the genus Eimeria. Pattern Recognit., 40, 1899–1910.

[6] Ginoris, Y. P., Amaral, A. L., Nicolau, A., Coelho, M. A. Z. and Ferreira, E. C. (2007a) Development of an image analysis procedure for identifying protozoa and metazoa typical of activated sludge system. Water Res., 41(12), 2581–2589.

[7] Ginoris, Y. P., Amaral, A. L., Nicolau, A., Coelho, M. A. Z. and Ferreira, E. C. (2007b). Recognition of protozoa and metazoa using image analysis tools, discriminant analysis, neural networks and decision trees. Anal. Chim. Acta, 595(1/2), 160–9.

[8] Widmer, K., W. and Srikumar, D., Pillai, S. D. (2005). Use of artificial neural networks to accurately identify cryptosporidium oocyst and giardia cyst images. Appl. Environ. Microbiol., 71(1), 80–84.

[9] Suzuki, C. T. N., Gomes J. F., Falcao, A. X. Papa, J. P. and Hoshino-Shimizu S. (2013). Automatic Segmentation and Classification of Human Intestinal Parasites from Microscopy Images. IEEE Transactions on Biomedical Engineering, 60 (3), 803-812.

[10] Tchiotsop, D., Saha T. B., Tchinda, R. and Kenné G. (2014). Edge detection of intestinal parasites in stool microscopic images using multi-scale wavelet transform. SIViP, DOI 10.1007/s11760-014-0716-6.

[11] Saha T. B., Tchiotsop, D., Tchinda, R. and Kenné G. (2014). Automated Extraction of the Intestinal Parasite in the Microscopic Images using Active Contours and the Hough Transform. Current Medical Imaging Reviews. In press.

[12] Golemati S., Stoitsis J., Sifakis E., Balkizas T., Nikita K. (2007). Using the Hough transform to segment ultrasound images of longitudinal and transverse sections of the carotid artery. Ultrasound in Medicine & Biology; 33 (12):1918–32.

[13] Stoitsis J., Golemati S., Kendros S., Nikita K.S. (2008). Automated detection of the carotid artery wall in B-mode ultrasound images using active contours initialized by the Hough transform. In: Conf. Proc. IEEE Eng. Med. Biol. Soc. 3146-9.

[14] Nixon, S. M. and Aguado, A. S. (2012). Feature extraction and image & processing for computer vision, third edition. Academic Press, Elsevier.

[15] Theodoridis, S. & Koutroumbas, K. (2010). An introduction to pattern recognition: a MATLAB approach, 5th ed.,. Academic Press, Elsevier.

[16] Engelbrecht, A.p. (2007). Computational Intelligence an Introduction, (2nd ed.).. John Wiley & Sons Ltd, The Atrium, Southern Gate, Chichester.

[17] Jollife, I.T., (1986). Principal Component Analysis. Springer-Verlag, New York.

[18] Sumathi, S. and Paneerselvam, S. (2010). Computational intelligence paradigms theory and applications using matlab. CRC Press, Taylor & Francis Group.

[19] Adhikari, A.; Adhikari, J. ; Pedrycz, W. (2014). Data Analysis and Pattern Recognition in Multiple Databases. Intelligent Systems Reference Library, Vol. 61. Springer International Publishing, Switzerland.

[20] Kasabov, N.K. (1998). Foundations of Neural Networks, Fuzzy Systems, and Knowledge Engineering, Second printing. A Bradford Book, the

Massachusetts Institute of Technology Press Cambridge, Massachusetts London, England.

[21] Hu, Y. H. and Hwang, J.N. (2002). Handbook of Neural Network Signal Processing. CRC PRESS LLC. Boca Raton   London   New York Washington, D.C.

[22] Hagan M. T., Demut, H. B. and Beale M. H. (2002). Neural Network Design

[23] Kramer, C.; Mckay B. and Belina, J. (1995). Probabilistic neural network array architecture for ECG classification. in Proc. Annu. Int. Conf. IEEE Eng. Medicine Biol., 17, 807–808.

[24] Mao, K. Z.; Tan K.-C. and Ser W. (2000). Probabilistic Neural-Network Structure Determination for Pattern Classification. IEEE transactions on neural networks, 11 (4), 1009-1016.

[25] Wu S.G., Bao, F. S., Xu, E. Y., Wang, Y., Chang, Y. and Xiang, Q. (2007). A Leaf Recognition Algorithm for Plant Classification Using Probabilistic Neural Network. IEEE International Symposium on Signal Processing and Information Technology.

[26] Demuth, H. and Beale, M. (2000). Neural Network Toolbox for Use with MATLAB.